UNIVERSIDADE Ð
COIMBRA

Carolina Flores Bugalho

IN VIVO CORTICAL AND SUBCORTICAL RECORDING
OF EYE MOVEMENTS-RELATED ACTIVITY IN
PARKINSON'S DISEASE

Dissertação no âmbito do Mestrado em Engenharia Biomédica, com especialização no ramo de Biomateriais, orientada pelo Professor Doutor Paulo Alexandre Vieira Crespo e Professor Doutor João Manuel da Fonseca Gomes de Lemos, apresentada ao Departamento de Física da Faculdade de Ciências e Tecnologia da Universidade de Coimbra.

Setembro de 2023

In Vivo Cortical and Subcortical Recording of Eye Movements-Related Activity in Parkinson's Disease

Carolina Flores Bugalho

Thesis submitted to the Faculty of Sciences and Technology of the University of Coimbra
for the degree of Master in Biomedical Engineering with specialization in Biomaterials

Supervisors:
Paulo Crespo (FCTUC and LIP)
João Lemos (CHUC and FMUC)

FCTUC, Physics Department
CHUC, Neurology Department

Coimbra, 2023

This work was developed in collaboration with:

"Technology has the potential to improve the quality of life for all, in ways we can only begin to imagine. "

\- Bill Gates

Agradecimentos

Em primeiro lugar, gostava de agradecer aos meus orientadores, Professor Paulo Crespo e Doutor João Lemos, sem os quais este projeto não teria sido possivel. Obrigada pelo entusiasmo e motivação, pela ajuda incansável e por tudo o que me ensinaram ao longo do último ano.

Quero agradecer a todas as pessoas envolvidas que desempenharam um papel fundamental no sucesso deste projeto. À equipa da Medtronic que me proporcionou, em primeira instância, esta oportunidade, em especial ao Engenheiro Miguel Dias e ao Engenheiro Gaetano Leogrande. Ao Doutor Ricardo Pereira, Doutor Fradique Moreira, Doutor Diogo Damas e Doutor Francisco Sales do serviço de Neurologia do CHUC. Ao Engenheiro Kurt Debono da equipa da EyeLink, Joel Cruz e José Gonçalves da equipa da Neuroevolution, ao Engenheiro César Teixeira e ao meu colega Francisco Cidade. Obrigada a todos pela ajuda, pelos conselhos e disponibilidade no decorrer deste trabalho.

Aos colegas e amigos que me acompanharam em todo o meu percurso académico desde a licenciatura em Lisboa ao mestrado em Coimbra, obrigada por terem feito destes anos, de facto, "os melhores anos da minha vida". Um obrigada especial às minhas amigas de todas as horas, Sofia e Inês, por ouvirem todos os meus lamentos e festejarem todas as minhas conquistas e ao Marcos, pelo suporte e amor constante.

Obrigada aos meus amigos de infância por crescerem comigo, por me apoiarem em tudo e por estarem presentes no fim de mais uma etapa da minha vida.

Por fim, o maior e mais especial agradecimento vai para a minha família. O que alcancei até hoje foi graças ao vosso esforço, aos vossos ensinamentos, ao vosso amor e à confiança que sempre depositaram em mim. Serão para sempre os meus maiores exemplos.

Abstract

Parkinson's Disease (PD) is a rapidly growing global health concern linked to basal ganglia (BG) degeneration and loss of dopamine, resulting in impaired saccadic eye movements. Deep Brain Stimulation (DBS) seems to improve motor function by decreasing beta band potency, which is pathologically increased in PD.

The study aims to synchronize DBS and Eye Tracking (ET) signals using Electroencephalography (EEG) as a linking element to investigate subcortical activity in the subthalamic nucleus (STN) during saccades in a PD patient. This new approach aims to provide new insights into ocular motor networks, normal and PD related patterns, and the effects of DBS.

A 69-year-old PD patient with predominantly right bradykinesia and implanted IPG- Percept™ PC underwent horizontal and vertical prosaccades. Transistor-transistor logic (TTL) signals were used to synchronize Eyelink and EEG systems by detecting common event markers. For Percept™ PC data, the correspondence was established through DBS artifacts sent to the EEG. Saccadic behavior, STN beta band potency and local field potentials (LFP) amplitude were analyzed during DBS on and off periods, using the Kruskal-Wallis, Mann-Whitney, ANOVA and Spearman tests. A p value less than 0.05 was considered significant.

After achieving the systems temporal synchronization, the analysis revealed that with DBS off, vertical saccades had lower velocity and gain compared to horizontal ones and, with DBS on, the gain of leftward saccades was increased and the latency of vertical saccades was shortened.

Furthermore, with DBS off, the right hemisphere beta band potency was lower during leftward (contralateral) than rightward saccades, while the left hemisphere, showed no significant difference between the two directions. Moreover, DBS was able to reduce left hemisphere beta band potency during rightward (contralateral) saccades when compared to DBS off. Additionally, left hemisphere beta band potency correlated positively with the gain of rightward saccades, with DBS on. No significant beta band differences were found for upward/downward saccades. LFP results roughly matched beta band potency results.

Synchronizing DBS with ET allowed the study of saccade generation in the subcortical network in vivo. With this innovative approach we were able to provide important insights into the probable normal (lateralized) ocular motor-related STN activity and the effect of DBS on restoring such activity in the presumably more affected STN.

Resumo

A doença de Parkinson (DP) é uma preocupação global no campo da saúde, associada à degeneração dos gânglios da base (BG) e à perda de dopamina, prejudicando os movimentos oculares sacádicos. A estimulação cerebral profunda (Deep Brain Stimulation, DBS) melhora a função motora, diminuindo a potência da banda beta, que está aumentada de forma patológica na DP.

Este estudo teve como objetivo sincronizar os dados da DBS e do rastreador ocular (Eye Tracking, ET) utilizando eletroencefalografia (EEG) como elemento de ligação, para investigar a atividade subcortical no núcleo subtalâmico (subthalamic nucleus, STN) durante a execução de sacadas num paciente com DP. Esta nova abordagem pretende fornecer novas perspetivas sobre as redes dos movimentos oculares, sobre os efeitos da DBS, e detetar padrões tanto normais como associados à DP.

Um paciente de 69 anos com DP, com predomínio de bradicinesia à direita e com IPG-Percept™ PC implantado, foi submetido à execução de prosacadas horizontais e verticais. Para a sincronização, sinais Transistor-transistor logic (TTL) foram enviados para o Eyelink e para o EEG para detectar marcadores de eventos comuns. No caso do Percept™ PC, essa correspondência foi feita através de artefatos da DBS enviados ao EEG. O comportamento sacádico, a potência da banda beta do STN e a amplitude dos potenciais de campo local (Local Field Potentials, LFP) foram analisados durante os períodos com DBS ligada e desligada, usando os testes de Kruskal-Wallis, Mann-Whitney, ANOVA e o procedimento de Spearman. Um valor de p menor que 0.05 foi considerado significativo.

Após alcançar a sincronização temporal dos sistemas, a análise revelou que, com a DBS desligada, as sacadas verticais apresentaram menor velocidade e ganho em comparação com as horizontais, e com a DBS ligada, o ganho das sacadas para a esquerda aumentou e a latência das sacadas verticais diminuiu.

Além disso, com a DBS desligada, a potência da banda beta no hemisfério direito foi menor durante as sacadas para a esquerda (contralaterais) do que para a direita, enquanto o hemisfério esquerdo não mostrou diferença significativa entre as duas direções. Com a DBS ligada, a potência da banda beta do hemisfério esquerdo foi reduzida durante as sacadas para a direita (contralaterais) em comparação com a DBS desligada.

A potência da banda beta do hemisfério esquerdo correlacionou-se positivamente com o ganho das sacadas para a direita com a DBS ligada. Por outro lado, não foram encontradas diferenças significativas na banda beta para sacadas para cima/baixo. Os resultados dos LFP coincidiram aproximadamente com os resultados da potência da banda beta.

A sincronização da DBS com o ET permitiu estudar a execução de sacadas na rede subcortical em tempo real. Esta abordagem inovadora forneceu perspetivas importantes sobre a provável atividade do STN relacionada com os movimentos oculares normais (lateralizados) e o efeito da DBS na restauração dessa atividade no STN presumivelmente mais afetado.

Palavras-chave – Sacadas, Gânglios da Base, Estimulação Cerebral Profunda, Doença de Parkinson, Movimentos oculares, Rastreador ocular, Eletroencefalografia, Potenciais de campo local, Núcleo Subtalâmico

List of Acronyms

LR Linear regression. 18

MCA Morphological Component Analysis. 18
MRI magnetic resonance imaging. 5, 55

PCCR Pupil Center Corneal Reflection. 14
PD Parkinson's Disease. xi, 1, 2, 3, 4, 5, 7, 8, 9, 11, 14, 16, 17, 20, 22, 23, 25, 27, 29, 32, 46, 55, 57
PSD Power spectral density. 8, 24

SN substantia nigra. 3
SNc substantia nigra pars compacta. 3
SNr substantia nigra pars reticulata. 3
STN subthalamic nucleus. xi, 3, 6, 7, 8, 19, 20, 22, 23, 24, 25, 46, 55
SVD singular value decomposition. 18, 19
SWJ square wave jerk. 14

TTL Transistor-transistor logic. xi, xiii, 21, 27, 28, 31, 35, 36, 37, 38

UDWT undecimated discrete wavelet transform. 18
UPDRS Unified Parkinson's Disease Rating Scale. 5

List of Figures

List of Tables

Contents

Contents

1

Introduction

This chapter contains the context and motivation (Section 1.1) and the expected goals (Section 1.2) underlying the present work. Section 1.3 briefly outlines the structure of this document.

1.1   Context and Motivation

Globally, disability and death due to Parkinson's Disease (PD) are increasing faster than for any other neurological disorder and, despite all the research that has been done, there is the need to optimizing diagnosis and treatment of PD [1].

PD is a neurodegenerative disorder characterized by focal degeneration of basal ganglia (BG), ultimately leading to severe loss of dopamine in the brain. PD is associated with slowing of body movements (i.e., bradykinesia), including eye movements [2] [3].

Eye movements in PD are characteristically impaired, possibly due to malfunction of the BG controlling ocular motor behavior. As an example, saccadic eye movements (i.e., rapid eye movements) are shortened in length (decreased amplitude, hypometric), slowly executed (decreased velocity) and initiated (increased latency). The above impairments correlate with disease duration, motor impairment and cognitive status [4].

Advanced treatment options in PD include, among others, the Deep Brain Stimulation (DBS). DBS electrodes implanted in the BG can not only deliver electrical pulses to modulate or disrupt abnormal patterns of neuronal signaling, but also provide the unique ability to record local field potentials (LFP), characterized in frequency bands, that allow access to subcortical brain activity [5].

DBS has been shown to improve ocular motor performance, although their mechanism has not been fully elucidated [6]. DBS appears to reduce/desynchronize the strength of beta band activity linked to motor functions, which is thought to reflect the neural activity of gangliobasal populations. Importantly, beta band potency seems to be pathologically increased/synchronized in PD and its level seems to correlate with the level of motor impairment [7]. Specifically in eye movement research, this has been shown in only one study so far, using data from intra-operatory electrodes during DBS placement, while a PD patient was performing an ocular motor protocol [7].

Eye Tracking (ET) is the current standard for accurately measuring eye movements. ET tracks the position and movements of the eyes, non-intrusively, through an infrared light source and converts it into a data stream containing oculomotor information. Also, response time, latency, and kinematics can be measured from eye movements, reflecting complex cognitive information [8].

Additionally, Electroencephalography (EEG) measures cortical activity, and its electrodes can also capture eye movement-related brain activity. Although most of this activity is believed to represent artifacts of eye muscles and not intrinsic neuronal activity, this system can function as a synchronization element [9].

1.2 Main Goal

In this pilot project, we aimed to measure in vivo subcortical eye movements-related activity of a PD patient by using synchronized data from DBS, EEG, and ET during an eye movement paradigm.

The brain network responsible for generating eye movements is complex, and its conceptualization is largely based on lesion studies. In contrast, this project goal was to study the brain activity during the execution of eye movements, which represents a unique opportunity to deepen our knowledge on eye movements network, its function in normal individuals and PD, and the influence of therapies such as DBS.

1.3 Document Structure

This document is organized into six chapters, in addition to the Introduction, as it follows: In Chapter 2, important concepts are described to understand the work performed and a literature review is made. In Chapter 3, the materials and methods used for this thesis are reported and analyzed. The results of the study are presented in Chapter 4, as well as their interpretive analysis. Finally, Chapter 5 presents the discussion and conclusions and Chapter 6 addresses future perspectives in this field.

2

State of the Art

This chapter introduces the main concepts needed to follow this document. Starting with a brief overview of Parkinson's Disease (PD) (Section 2.1), moving on to Deep Brain Stimulation (DBS) (Section 2.2), Eye movements and Eye Tracking (ET) system (Section 2.3) and Electroencephalography (EEG) (Section 2.4). In Section 2.5, a review of some literature on the topic at hand is conducted, presenting an overview of the current State of the Art.

2.1   Parkinson's Disease

PD is a progressive neurodegenerative disorder characterized by slowness of movements (i.e., bradykinesia), muscular rigidity, tremor, imbalance (i.e., loss of postural reflexes) and other complications including cognitive impairment, mood disorders, sleep disorders, and pain [2]. In addition, PD is involved with a disturbance of eye movements. Both reflexive and voluntary eye movements are impaired, resulting in saccadic hypometry, decomposed pursuit, decreased accuracy, and increased latency of movements [10].

PD is associated with focal degeneration of brain areas involved in the generation of more voluntary movements, including the basal ganglia (BG) in the subcortex, ultimately leading to a severe loss of dopamine neurons in the brain. Dopamine acts as a chemical messenger between the parts of the brain and nervous system that help control and coordinate body movements [11].

The BG consist of four main nuclei: the striatum (constituted by the putamen and the caudate) that represents the main "input" region in the whole of the basal ganglia; the globus pallidus (GP), divided into internal globus pallidus (GPi) and external globus pallidus (GPe) portions; the subthalamic nucleus (STN) and the substantia nigra (SN), formed by the substantia nigra pars compacta (SNc) (mostly composed of dopaminergic neurons) and substantia nigra pars reticulata (SNr), which, together with the GPi, form the main "output" structure of these ganglia (Figure 2.1) [12].

PD is characterized by a gradual decrease in SNc activity, resulting in a decrease in secreted dopamine. There are two types of dopaminergic receptors, D1 (excitatory type) and D2 (inhibitory type) that influence motor activity. The loss of dopamine in the striatum of PD patients results in increased activity in the GPi/SNr circuits and subsequent gamma-aminobutyric

acid (GABA) dysfunction, leading to inhibition of the thalamus. The result is a decreased ability of the thalamus to activate the frontal cortex, resulting in the decreased motor activity characteristic of PD (Figure 2.2). Consequently, restoration of dopaminergic activity in the striatum through activation of D1 and D2 receptors with dopaminergic therapies mediates clinical improvement in the motor symptoms [13] [14].
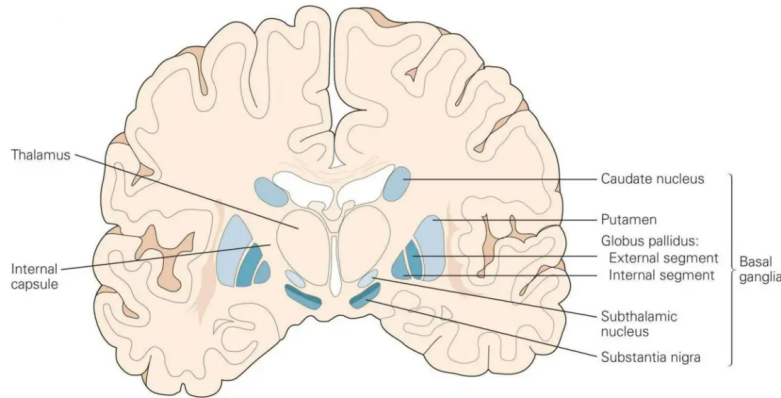
Figure 2.1: Coronal section of BG in the human brain. Adapted from [15].
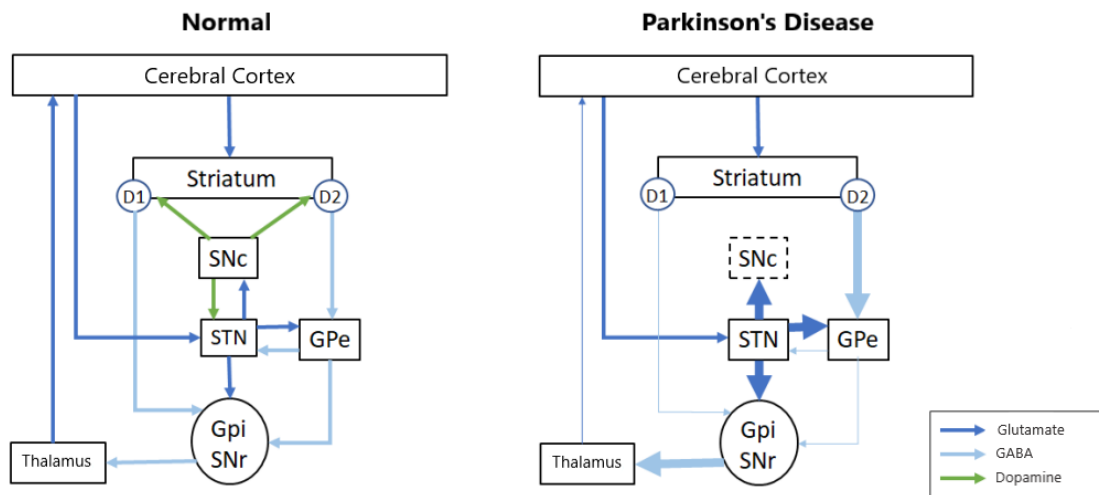
Figure 2.2: Diagram illustrating the organizational circuitry of BG under normal conditions compared to PD conditions. The thickness of the arrows is proportional to the activation of the transmission pathways. Adapted from [14].

Nowadays, PD is the second most common neurodegenerative disorder of aging and the most common movement disorder, with a global prevalence of more than 8 million individuals, which is expected to increase 50% by 2030 [16] [17].

The causes of PD are not fully understood, but a combination of genetic and environmental factors is likely involved. The average age of diagnosis is around 55 to 65, however about five to ten percent of patients are diagnosed before the age of 50 [18].

When a patient is suspected of having PD, the diagnosis is essentially clinical, based on the presence of characteristic motor symptoms (mainly bradykinesia, tremor or rigidity), by which patients are classified according to the Unified Parkinson's Disease Rating Scale (UPDRS) [19]. There are no specific tests that diagnose PD, however, certain structural neuroimaging tests of the brain, such as magnetic resonance imaging (MRI) (excludes structural lesions) or Dopamine transporter imaging with single-photon emission computed tomography (DAT-SPECT) (acts as a marker of the dopamine level), can be used to support the diagnosis or to exclude other neurological conditions [20].

The clinical expression of PD symptoms is variable, as is the progression of the disease and response to therapy. Among the therapies currently available to help relieve the symptoms and maintain PD patients quality of life are supportive therapies like physical and speech therapy, dopaminergic drugs (e.g., levodopa, dopamine agonists or monoamine oxidase-B inhibitors), used to restore depleted dopamine levels, and more recently, surgery involving DBS (Section 2.2) [21].

Importantly, both dopaminergic drugs and DBS have been shown to improve not only voluntary body movements, but also eye movements (Section 2.3) , possibly due to their action on regaining part of normal BG activity [22].

However, the most recognized complications in PD, such as motor fluctuations and dyskinesias (i.e. involuntary muscle movements), might be related to the above therapy, believed to reflect excessive/unwanted activation of the cells that produce dopamine. Therefore, there is still no therapy that can effectively delay or completely reverse PD [23].

2.2 Deep Brain Stimulation

In advanced stages of PD, when medications no longer adequately control motor symptoms, DBS offers a powerful therapeutic alternative. It is a surgical therapy involving the implantation of electrodes into specific regions of the brain, which deliver electrical stimuli to modulate or disrupt abnormal patterns of neural signaling within the targeted region [5].

DBS was first used in 1987 to treat tremors in PD (Benabid et al., 1987) [24], receiving US Food and Drug Administration (FDA) approval in 2002. Since then, DBS has evolved greatly and has been used to treat over 40,000 people with PD worldwide [25].

Patient selection, surgery, post-operative stimulator programming, and patient care throughout the process require a multidisciplinary team. Also, DBS as a treatment is only indicated for about one in three PD patients, since it only works for certain stages of the disease, with specific symptoms related to specific brain circuits. Usually, it is approved for people who have had PD for at least four years and who still benefit from medication but have motor complications, such as significant "off" time (i.e., periods when symptoms return because the medication is not working well) or dyskinesia. DBS typically works best to lessen motor symptoms of stiffness, slowness and tremor and it's not recommended for people with dementia [26].

Typically, each electrode has four contacts and from these contacts result six pairs (i.e. six different results for each electrode: 0-3, 0-2, 0-1, 1-2, 1-3, 2-3, for a total of twelve different results), as shown in Figure 2.3. In this case the study is done with the Medtronic Lead model 3389, which is compatible for movement disorders, although there are different and more recent models available in the market.
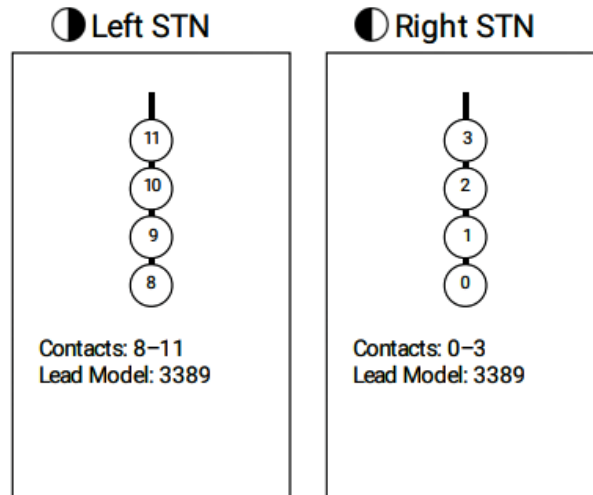
Figure 2.3: DBS lead configuration example for both right and left hemispheres in the STN. Source: [27].

The best contact and best parameters are different for different patients. The electrodes are connected by an extension, which goes under the skin from the head to the upper chest, and connects them to a neurostimulator (i.e., implantable pulse generator, sometimes called a "brain pacemaker") that produces the electrical pulses needed for stimulation (Figure 2.4). The pulses can be adjusted remotely to check or modify the neurostimulator's settings [28].

Figure 2.4: Concept and Assembly of DBS device. Source: [28].

There are three main surgical sites for PD treatment: the STN, the GP and the thalamus (Figure 2.5). Surgery is most commonly performed in the STN and the GP, on either one side or both sides of the brain. In these locations, DBS can significantly improve all the major motor features of PD, including bradykinesia, rigidity, tremor, and, to a certain extent, gait. On the other hand, surgery in the thalamus improves only tremor. When surgery is performed on one side of the brain, the major benefit is seen on the opposite side. Some patients may require only surgery on one side of the brain whereas other patients may require bilateral surgery [29] [30].

Figure 2.5: Surgical placement of DBS leads. (a) Anatomical directional terms. Sagittal section of the (b) STN position, (c) thalamus position and (d) GP position for lead implantation. Adapted from [31].

DBS surgery offers a unique opportunity to record local field potentials (LFP), the electrophysiological population activity of neurons surrounding the depth electrode in the target area. With access to the subcortical activity, LFP research has offered valuable insight into PD mechanisms and cognitive processes and inspired the advance of adaptive DBS [32].

LFP have been characterized in frequency bands (Hz): delta (0-3), theta (4-7), alpha (8-12), beta (13-30) and gamma (31-200) and high frequency (> 200), although literature related to oscillatory activity in the BG broadly describes beta band in the 8 to 30 Hz range [33].

While activity changes in each frequency band contribute to normal processing in the brain, persistent activity in the beta frequency range in the STN has been associated with lead placement, discontinuation of antiparkinsonian medications and recurrence of symptoms, particularly bradykinesia and rigidity. Beta LFP are attenuated with stimulation and medication (Figure 2.6). In contrast, the appearance of frequencies in the gamma range in the BG may be related to the effort of a motor response. Thus, higher stimulation amplitude may induce gamma oscillations. These factors may influence LFP signals and justify the observed variability between patients [33].

Figure 2.6: LFP recordings, under different conditions, with the Percept™PC device in a patient with PD. Power spectral density (PSD) specifies the power levels of the frequency components present in a signal, showing a peak in the beta frequency range with stimulation and medication OFF. Adapted from [33].

Also, since the STN is the part of the BG circuit that controls saccadic eye movements (Section 2.3) the effects of beta oscillations are also related to these movements [34].

Over the years, several studies have demonstrated an overall improvement in patient quality of life with a significant reduction in medication, motor scores, increased "on" time by six hours per day, reduced dyskinesias by 80 to 90%, and reduction of "wearing off" in patients who have implanted DBS (Figure 2.7) [35].
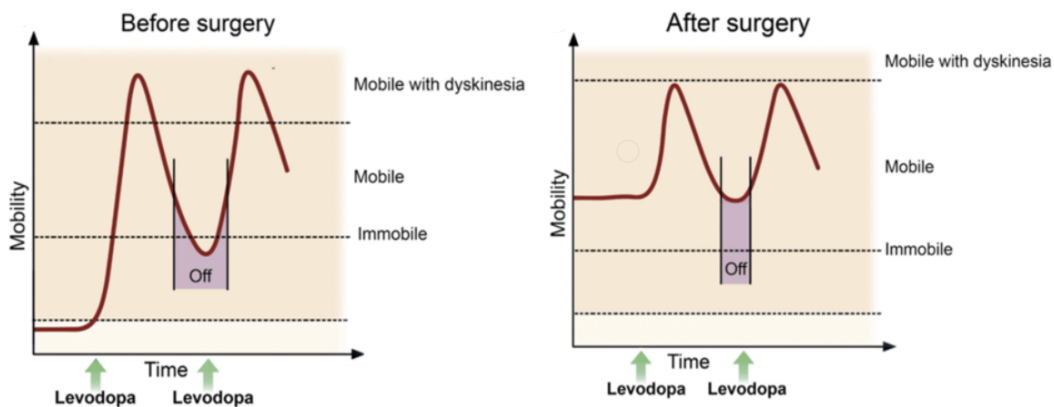
Figure 2.7: Mobility and motor function before and after DBS surgery. Source: [36].

2.2.1   Percept™ PC

Medtronic is a pioneer in DBS, developing the Percept™PC device, which has been upgraded recently with BrainSense™ Technology, allowing for real-time capture of brain signals in the BG, while not compromising the delivery of electrical pulses to the aforementioned structures.

To date, Percept™PC operates with open-loop stimulation but it is expected that in the

next few years it will move fully to closed-loop stimulation. As demonstrated in Figure 2.8, in open-loop DBS (a), the stimulation is continuous, has a fixed amplitude, and there is no correct connection between the input and output signal. The clinician sets parameters that provide the input to the controller, which provides the stimulation [37].

On the other hand, in closed-loop DBS, Figure 2.8 (b), the output of the controller depends on the input signal. Multiple input variables carry multiple output variables, allowing changes in the input to lead to changes in the output. It works by measuring either brain activity (e.g., an EEG) or a specific behavior (e.g., tremor) and automatically changing the stimulation based on that measurement (e.g., more current) until the wanted result is achieved. In this case, the power, duration or shape of oscillations could be input variables detected by the controller, which delivers stimulation with parameters that are continuously adjusted to match the changes in input variables and to match beta power [38].
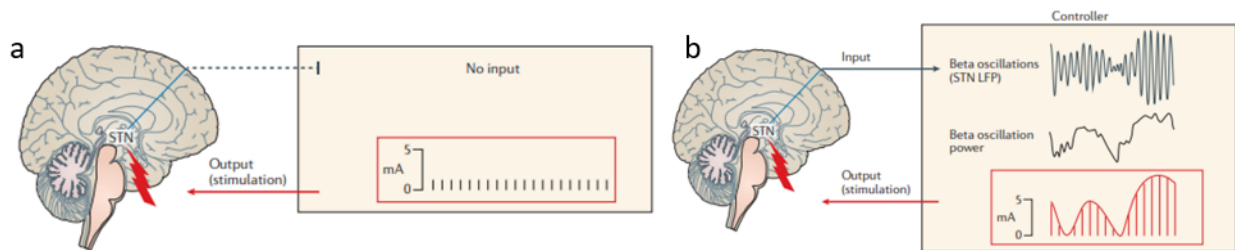
Figure 2.8: Current DBS system designs: (a) Open-loop DBS and (b) Closed-loop DBS. Adapted from [38].

In this way, the patient's clinical status is quantified and used to change the stimulation parameters as needed, thus reducing possible stimulation-induced side effects while controlling symptoms, ultimately aiming for a personalized treatment strategy. Additionally, the use of Percept™ technology can also help to unravel the mechanisms underlying the disruption of eye movements in PD and those associated with treatment responses [39].

Medtronic's Percept™PC neurostimulator with BrainSense™ technology is designed to capture a patient's brain signal to understand the impact of treatment decisions, medication changes, or stimulation. To date, the Percept™PC for PD is the only commercially available DBS device with sensing technology, that captures LFP, records and stores in the device while applying therapeutic stimulation. LFP is typically used with micro-electrodes, differentiating from EEG (Section 2.4) , which is recorded on the surface of the scalp, and with macro-electrodes [40] [41].

Allied to this technology is also an event monitor (Figure 2.9), which creates opportunities for real, everyday data acquisition. Patients can monitor up to four predefined PD events (e.g., medication adherence, adverse effects and symptoms) in their scheduler, and the clinician can correlate them with BrainSense™ data [40].

Figure 2.9: Percept™ PC device. (a) Patients programmer; (b) Clinician programmer; (c) Neurostimulator. Adapted from [42].

The first step in setting up BrainSense™ technology is to use the BrainSense™ Survey (Figure 2.10), which is performed with stimulation off and produces a plot of the difference in LFP signal between any two pairs of contacts. These data are automatically processed through fast Fourier transform (FFT) and presented as LFP magnitude (Vp, microvolt peak) versus beta band frequency (Hz) for each of the contact combinations.

This survey allows viewing of the entire spectrum in the frequency range (0-125 Hz), allowing the clinician to determine if a signal is detectable and from which contact pairs. The contact pair with the highest beta magnitude is selected for stimulation (activating one of these two contacts). In this region is expected the highest electrophysiological activity potential difference and consequently the greatest benefit and capacity for symptomatic control of the stimulation [41] [43] .
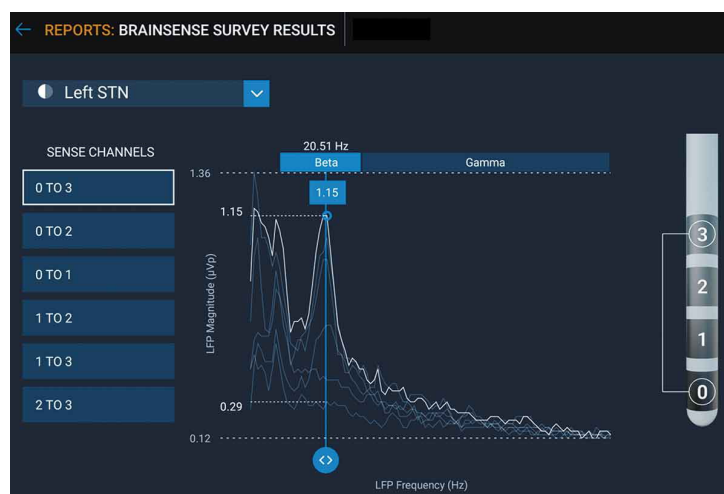
Figure 2.10: Lead Impedance and results recorded during a human BrainSense™ Survey. Source: [27].

The Brainsense™ Setup is used to activate a specific contact for stimulation. In order to prevent any interference or unwanted signals, the two detection contacts are positioned at an equal distance from the stimulation contact. There are only 3 possible configurations for this, as demonstrated in Figure 2.11:
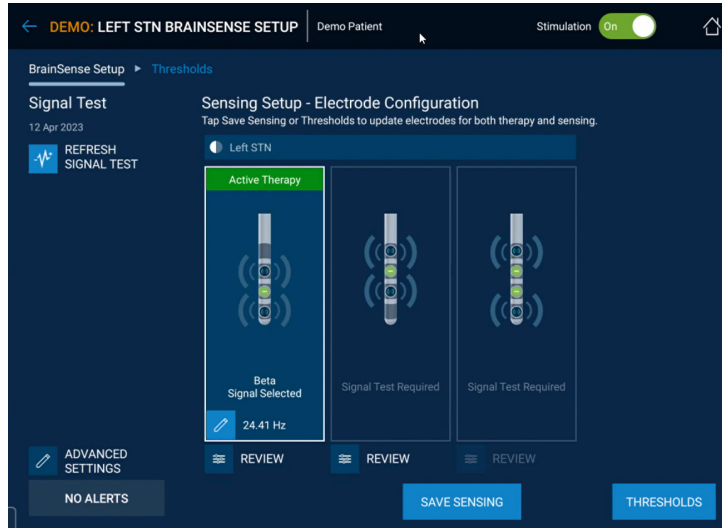
Figure 2.11: Possible lead configurations during a BrainSense™ Setup test. Source: [27].

Once BrainSense™ Setup is complete, the user can view LFP power in a selected frequency band and with the selected contacts in real time by streaming the data to the clinician's tablet. This is used to monitor changes in LFP during active stimulation programming or while guiding and observing the patient performing activities (e.g., eye movement tasks).

The tablet displays the selected power and stimulation amplitude in real time and over the entire recording. Increasing stimulation amplitude resulted in a decrease in beta-band power (Figure 2.12). In addition, Brainsense™ Streaming can be used to collect time domain data from the selected channel(s) for offline analysis and signal processing [33] [40].
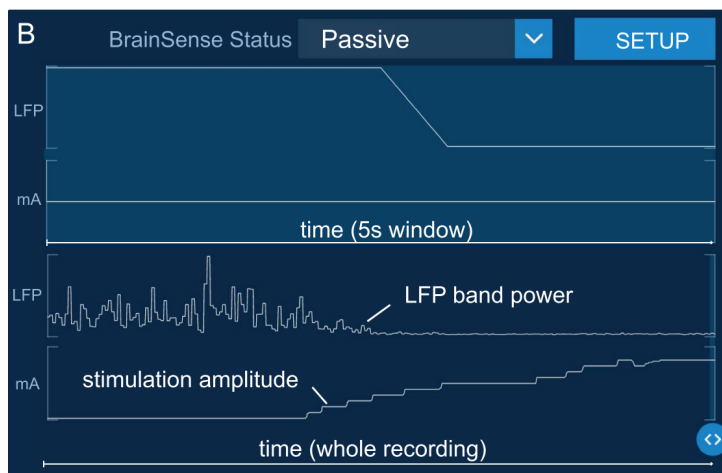
Figure 2.12: An example of power tracking in a selected frequency band in BrainSense™ Streaming mode on a patient with PD. Source: [27].

2.3 Eye Movements and Eye Tracking

Eye movements serve to stabilize the gaze and keep the image stable on the retina, as well as to direct the gaze to an object of interest. Eye movements can be divided into several types, each of which is controlled by a specific neural pathway that converges at the level of the ocular motor nuclei in the brainstem [44]. The neural circuits that control eye movements are complex and distributed in cortical areas (mainly frontal and parietal) and subcortical structures (BG, midbrain, brain stem, thalamus, and cerebellum), as shown in Figure 2.13.
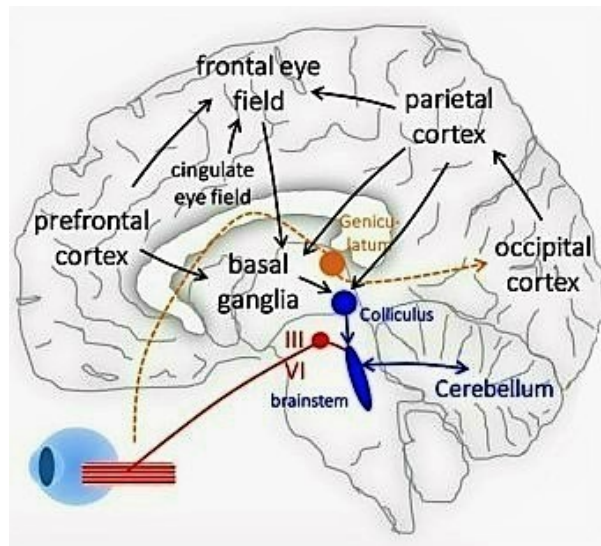
Figure 2.13: Schematic overview of important cortical and subcortical regions involved in the control of eye movements. Arrows indicated the propagation of information. Adapted from [45].

The control of eye movements by the brain is a complex and intriguing process that scientists have been trying to study for the last years. It is known that when we move our eyes to the right, the left hemisphere of the brain is primarily involved. Similarly, the right hemisphere controls eye movements to the left. However, when it comes to eye movements in the up and down directions, both hemispheres seem to play a role. Although researchers have made progress in understanding the brain regions responsible for eye movement control, there is still much more to uncover.

Saccades and pursuit are examples of reflexive eye movements, whereas fixation and antisaccades are examples of more voluntary eye movements. Saccades are rapid eye movements that redirect gaze to place the image of an object of interest in the central area of the retina, where photoreceptor density is highest and visual acuity is best. Antisaccades are a type of saccade in which the gaze is directed in the opposite direction of a sudden movement [44] [46].

In contrast, eye movements in smooth pursuit are much slower and allow us to hold a moving object still, and eye fixation is the point between two saccades where the eyes are relatively immobile. It consists of small eye movements (i.e., microsaccades, ocular tremor, and drift) that appear to prevent fading and further stimulate visual tracking mechanisms [44] [46].

Analysis of eye movements can provide objective and quantifiable information about the quality, predictability, and consistency of movements. They can be precisely quantified in terms of their amplitude, frequency, latency, gain, speed, etc [47]. These metrics of oculomotor behavior can be obtained from fixations, saccades and smooth pursuit (Table 2.1).

Table 2.1: Summary of possible oculomotor measurements.

Eye Movement Measurements		
Fixation	**Saccades**	**Smooth Pursuit**
Count	Amplitude	Direction
Duration	Duration	Velocity
	Velocity	Acceleration
	Latency	Latency
	Rate	Gain
	Gain	

Particularly in saccades, the distance a saccade travels during an eye movement is defined as amplitude. It is expressed in visual degrees (angular distance) or pixels. Saccade velocity is calculated using the first derivative of the time series of gaze position data, while peak saccade velocity is the highest velocity reached during a saccade. Saccade latency measures the duration between the onset of a stimulus and the onset of the saccade. In a healthy person, latency is about 100 ms and is linearly related to amplitude and velocity for a prosaccade of up to 10°. For antisaccades, the latency is about 300 ms and the amplitude is 30° [48].

Also, the number of saccadic eye movements per unit time is called saccade rate (or saccade frequency), and the ratio of initial saccade amplitude to target amplitude is known as saccade gain (or saccade accuracy). This metric measures how well a saccadic movement landed on the target stimuli [47] [49].

Figure 2.14 schematically represents the ocular metrics discussed above.
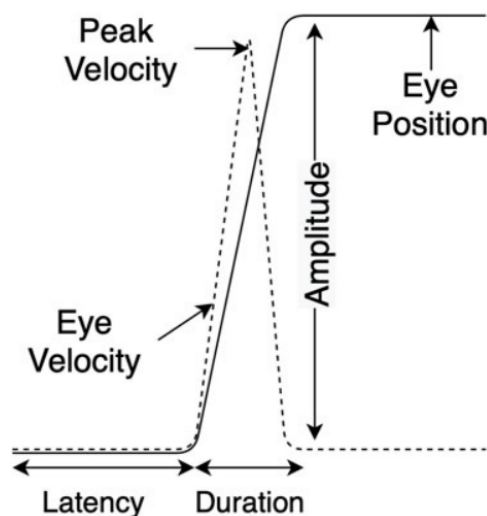
Figure 2.14: Schematic representation of the common saccade metrics. Adapted from [47].

Different paradigms have been used to understand stages of information processing when subjects perform different tasks and how impaired circuitry manifests itself in behavior in clinical conditions like PD [50]. Not surprisingly, eye movements are impaired in PD, with unstable ocular fixation, decomposed ocular pursuit, and difficult-to-initiate saccades (i.e., prolonged latency) that often undershoot the visual target (i.e., hypometric).

PD patients show also unusually frequency, poor convergence ability, and large square wave jerk (SWJ) (i.e., saccadic intrusions, usually 0.5–5°, that move the eye from and back to the fixation point with an intersaccadic interval of about 200 ms) [51] [52].

ET is the current standard system to measure eye movements. The accuracy and high sampling rates in this system, allows for the detection of subtle differences in core oculomotor metrics used to evaluate ocular fixation, ocular pursuit, and saccades.

Monitoring eye movements in people with PD reveals important information about an individual's cognitive and motor function and provides a sensitive method of diagnosing and monitoring the course of the disease, using several eye scans from the same patient [53].

ET works by following the eye position and movements, non-intrusively, with a source of infrared light that illuminates the pupil. Thus, a reflection generates on the cornea, and an infrared camera will then record it, delimit the center of the pupil, deduce eye rotation, and determine gaze direction. Pupil Center Corneal Reflection (PCCR) is the main method ET uses, in which the pupil and corneal reflections are optically monitored (Figure 2.15). After that, the recorded information becomes raw data that ET software subsequently processes [54].
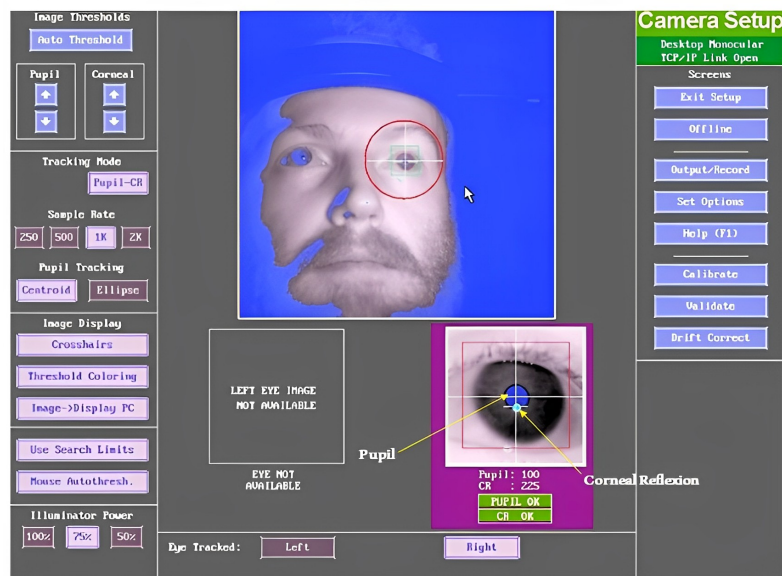
Figure 2.15: ET Participant Setup. Adapted from [55].

2.3.1 EyeLink 1000 Plus

In this work, we used the EyeLink 1000 Plus (Figure 2.16), one of the most accurate and precise video-based ET in the world, sampling binocularly at up to 2000 Hz. ET like EyeLink use single cameras that can capture up to 2000 images of both eyes every second. The system is highly customizable and versatile, with multiple mounting options, interchangeable lenses, modes for tracking the head with and without head fixation, and allows integration with EEG [56].

The ET software uses image processing algorithms to identify two key locations on each of the images sent from the camera: the center of the pupil and the center of the corneal reflection. Camera images are processed by software running on a dedicated host PC, using a real-time operating system to ensure excellent temporal precision. Gaze data is returned from the host PC to the stimulus presentation computer and other external devices via an Ethernet connection and/or analog voltage [56] [57].

Figure 2.16: EyeLink 1000 Plus equipment. Source: [55].

2.4 Electroencephalography

EEG is a simple, non-invasive test that evaluates the brain's electrical activity by recording it with electrodes placed on different parts of the scalp, more so at the cortical level, through the use of an electroconductive gel which reduce the existing impedance. It is very informative, allowing changes in the brain's electrical activity to be detected and recorded on a graph. The signal's spatial resolution is determined by the number of electrodes used and their respective localization, while time resolution depends on the sampling frequency [58].

Scalp EEG is the most common acquisition method because it is noninvasive. The standard for electrode placement in adults consists of 21 electrodes and is referred to as the International 10-20 System (Figure 2.17), with rules for electrode placement based on percentages, directly related to these positions. Specifically, the letters represent the brain lobe/area (Fp - frontal polar, F - frontal, C - central, T - temporal, P - parietal, O - occipital), followed by an odd number for left, an even number for right, or the letter z for midline electrodes [58] [59].
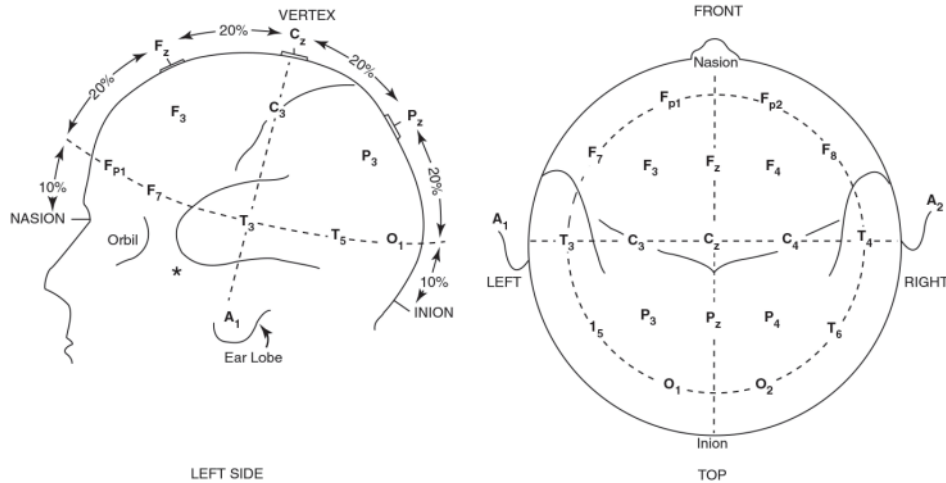
Figure 2.17: The International 10-20 System used for scalp electrodes placement. Source: [59].

Each EEG signal, usually referred to as a channel, measures the voltage difference between two electrodes. These electrode arrangements result in different configurations as referential and bipolar montages. When acquiring the signal with a referential assembly, each electrode measures the voltage difference between the electrode itself and a reference. After acquisition, one can either keep the original signals or create so-called bipolar montages, which typically use the difference between the voltages measured by adjacent electrodes [59].

In this case, the EEG used in the study belongs to Neuroevolution. It is very powerful and versatile, and provides high quality signal integrity and durability. It includes a camera to record the entire process and the SD PLUS™ amplifier, which is available in a variety of configurations to suit any application, from routine EEG studies to clinical research [60].

Normal oscillations are divided into bands according to frequency width, and it is one of the most studied EEG features in PD patients. For example, studies have shown that cognitive deficits are correlated with a slowing of EEG frequencies. In addition, EEG may reveal abnormalities of dopaminergic subcortico-cortical circuits in patients with PD. Conventional time-frequency analysis of EEG signals can provide further insight into the disrupted sensorimotor networks at PD, but cannot fully reveal the nonlinear processes of neural activity and interactions [61].

Information about eye movements is also recorded. The patterns of cortical neuronal activity associated with visual attention and saccade execution have also been shown to occur in eye movement tasks once the contribution of eye and eyelid movements to the signal measured on the scalp has been artifact-adjusted. Thus, the EEG proves to be a fundamental element of synchronization with the ET [9].

2.5 Related Works

In recent years, the scientific community has witnessed the publication of significant reports pertaining to innovations and discoveries in the field of eye movements and/or DBS for patients with PD or related pathologies, from studies of artifacts to the different methodologies and technologies used. These interdisciplinary approaches are expected to advance our understanding and potentially reveal new discoveries in this field of research.

2.5.1 Standardized Protocols for Quantification of Eye Movements

Current studies on eye movements usually focus on only one or a few aspects of oculomotor control and protocols differ considerably. In addition, there is a lack of transparency in data analysis, which often relies on device-specific ET software. This ambiguity limits the ability to critically evaluate the strengths and weaknesses of individual studies and consequently to develop a common approach, so it was quite necessary to come up with a solution.

In 2018, J. A. Nij Bijvank et al. [62] provided a standardized, open-source and transparent protocol for measuring and analyzing eye movements in a multicenter setting: DEMoNS (Demonstrating Eye Movement Networks with Saccades). The DEMoNS protocol details the resulting treatment trial measurements that are of excellent reproducibility and can be applied to the study of saccadic and fixational eye movements in various neurodegenerative and motor diseases, including PD. The algorithms efficiently and consistently calculated the parameters of interest such as peak velocity, latency, and gain, with good reproducibility.

However, there were still difficulties in collaboration between research groups hindering the translation of results into clinical practice. In 2023, a project conducted at Coimbra University [63], aims to bridge this gap between basic research and clinical applications by creating a standardized and accessible interface for the analysis of eye movements.

Based on the DEMoNS protocol, the software was designed to seamlessly integrate into the existing ET device (Eyelink SR Research, 1000Hz), providing real-time data acquisition and analysis capabilities. The interface offers flexibility for researchers to customize specific parameters while respecting the standardized framework, ensuring consistent and comparable results across diverse experimental settings.

2.5.2 Artifacts Affecting Data Accuracy

A relevant issue in this area under study are the artifacts caused by eye movements, with different time-frequency properties, into electroencephalographic recordings, which make data analysis difficult. Trials contaminated by eye movement, for example when blinking, have to be eliminated, which is why in standard EEG paradigms subjects are required to fixate on the screen.

To overcome this restriction some studies have been made, in particular one by Michael Plöchl et al. [9] that recorded eye movements from EEG channels during a guided eye movement

paradigm to explore artifact properties such as corneo-retinal dipole changes, saccadic spike potentials, and eyelid artifacts. In this process, it was necessary to calibrate eye movements and define saccades based on specific thresholds.

All data were preprocessed and analyzed in Matlab with FieldTrip and EEGLAB toolbox. EEG data were downsampled to 500 Hz to match the sampling rate of the eye data and low-pass filtered at 100 Hz. Eye and EEG data were then matched by slicing them into trials corresponding to triggers sent simultaneously to both systems. Finally, the EEG data were visually reviewed and trials with high amplitude noise were removed, typically resulting from muscle activity, as blinks.

The simultaneous EEG and eye movement recordings allowed for a comprehensive study of eye artifacts, their properties, and interrelationships, making the results more comparable. The results confirm that these artifacts come from different independent sources and that, depending on electrode location, gaze direction, and reference choice, these sources contribute differently to the measured signal. The researchers compared two artifact correction methods, Linear regression (LR) and Independent component analysis (ICA), finding that ICA was more effective in removing ocular artifacts, including microsaccadic spiking potentials, while preserving neural signals.

Another perspective from Balbir Singh et al. [64], proposed a systematic decomposition method called Morphological Component Analysis (MCA), which provides a form of reconstruction and ensures accuracy in decomposing the true EEG and electrooculography (EOG) signal, demonstrating that the most suitable waveforms combination for data analysis to represent their morphology was undecimated discrete wavelet transform (UDWT), discrete sine transform (DST), and DIRAC (i.e., standard unit vector basis).

When dealing with DBS patients, artifacts caused by the electrodes can be also problematic. One of the challenges is to separate the frontal lobe activity that is activated when we move our eyes from the local artifacts of the cranial retinal potential that can parasitize some electrodes. The most common artifacts in DBS recordings are Electrocardiography (ECG) artifacts from the heart's electrical activity, movement artifacts due to patient's involuntary movements, and stimulation artifacts caused by electrical pulses during therapy.

The source of ECG artifacts in DBS studies might be related to the positioning of the neurostimulator in relation to the heart, potentially causing partial overlap with the LFP signal in a specific frequency range, leading to signal distortions and erroneous readings and interpretations. Furthermore, some studies revealed that using monopolar settings for DBS can cause ECG artifacts, while they were not present when using bipolar settings or turning off the DBS. Interestingly, the location of the electrodes and the patients underlying disease did not seem to have any impact on the occurrence of these artifacts [65].

Usually, ECG artifact suppression methods are more sophisticated, and several approaches, such as QRS interpolation from the Perceive toolbox, template subtraction, and singular value decomposition (SVD), have proven to be effective. These methods successfully reduced artifact-

induced power in the beta frequency band, partly recovered beta peak and beta burst dynamics and are essential to distinguish genuine R-peaks from ECG artifacts (Figure 2.18). The SVD method was identified as the preferred option, striking a balance between cleaning artifacts and preserving neural signals [66].
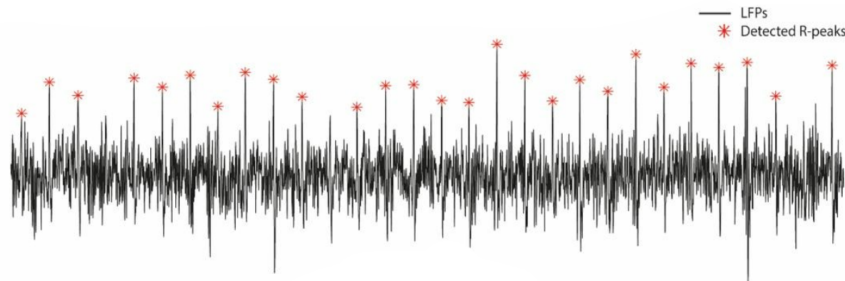
Figure 2.18: ECG artifact typical peaks (red asterisks) in a recorded LFP signal. Source: [66].

High-amplitude electrical signals from stimulation can make it hard to distinguish genuine neural activity. To solve this before data recording, researchers can use signal processing techniques and adjust stimulation settings to reduce artifacts while keeping the brain signals intact. Patient movements can also create unreliable data, so researchers use motion tracking systems or carefully design experiments to minimize such issues during recording sessions [67] [40].

In addition, there are several approaches to mitigate these artifacts, during the analysis process: filtering techniques such as notch, high-pass, low-pass and band-pass filters (Figure 2.19). ICA and blind source separation can be used to separate signals from multiple sources. Spatial filtering can be used to reduce the contribution of specific electrodes to the recorded signal, such as common average reference. The combination of these techniques can lead to more accurate measurement of activity of interest [68] [69] [70].
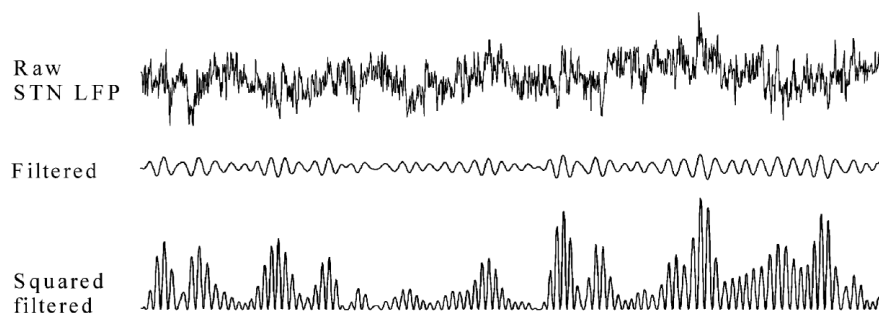
Figure 2.19: Representative example of raw LFP data recorded from left STN and the same data bandpass-filtered between 19Hz and 34Hz. After filtering, the resultant activity was squared, providing a dynamic measure of frequency band power, in order to emphasize oscillatory components in the data. Source: [71].

2.5.3 Deep Brain Stimulation and Eye Tracking: Overcoming the challenge of synchronization

The convergence of DBS and ET technologies holds great promise for medical advancements and scientific exploration. While DBS effects on motor function are better studied, its influence on eye movements remains largely unexplored. Implanting DBS in PD patients provides a unique opportunity to study its impact on eye movement behavior. Understanding how DBS influences eye movements is crucial due to their shared neural networks, which allows for valuable comparisons and interpretations of motor function and physiology.

In recent years, a number of studies have been conducted focusing on the influence of DBS on GP, STN, and thalamus on ocular and vestibular motor function. The results suggest that DBS in both STN and GP improves prosaccadic latencies. DBS in STN can enhance smooth pursuit in PD and modulate visuospatial attention, providing experimental evidence for a Bayesian model of BG function, while DBS in the GP can improve antisaccadic performance at PD, suggesting improvement in oculomotor control and implying retrograde stimulation of the striatum as part of the mechanism of action. Futhermore, a pathway exists from the vestibular nucleus to the striatum via the thalamus which contributes also to motor control [72] [73].

In 2021, Maja Klarendic et al. [22], discussed the application of DBS treatment in different diseases, how different stimulation sites interfere with known eye movement circuits and the consequent oculomotor and visual effects they can produce. DBS effects on eye movements vary in the literature, but understanding them is crucial due to the overlap with targeted networks.

The results on the effects of DBS on eye movements suggested that when targeting the GPi, DBS seems to enhance voluntary saccade parameters, particularly reducing antisaccadic error rates through positive modulation of higher oculomotor networks. On the other hand, stimulation of the STN can increase antisaccadic error rates, possibly due to disrupted STN-frontal connections crucial for saccadic inhibition, while improving specific parameters of visually guided saccades in PD. Ocular dysconjugacy with ipsilateral eye adduction and depression can occur due to STN DBS, potentially causing blurred vision or diplopia. Additionally, improper lead placement can lead to gaze deviations. Thalamic DBS interrupts projections to midbrain structures, potentially impairing smooth pursuit.

The conflicting results among studies reporting the effects of DBS on eye movements are likely related to differences in methodological approaches used, status of levodopa medication, as well as possible variability in DBS electrode placement, highlighting the need for more research with less common DBS targets on possible effects on eye movement, and including comparisons of uni- and bilateral stimulation, and hemispheric asymmetry in eye movement control in relation to DBS.

The best way to study the relationship of DBS to eye movements is to perform analysis with ET. While DBS and ET could potentially be used together to study brain function or evaluate the effectiveness of treatment, synchronizing these two systems would require careful planning and coordination, because they are separate technologies with their own specialized

hardware and software. To synchronize the two technologies, a specialized system would be required that can communicate with both systems and that can be programmed to coordinate the timing and delivery of electrical stimulation from the DBS device with the data collected from the ET system.

2.5.3.1   Integrating Deep Brain Stimulation and Electroencephalography

In order to synchronize data obtained from DBS with data from ET, a common synchronization element is usually needed, an EEG that is able to show signals from both systems. While DBS allows both recording of brain activity and stimulation of parts of the brain that are difficult to reach with noninvasive techniques, EEG provides complementary information from other areas of the brain that can be used to characterize the brain networks targeted by DBS. However, this requires careful consideration of the different types of artifacts in data acquisition and subsequent analysis. One of the major research directions is the simultaneous recording of LFP from DBS targets and EEG [74].

2.5.3.2   Combining Eye Tracking and Electroencephalography

The combination of ET and EEG is one of the most fascinating and difficult problems in this field of research. ET alone is not enough, as it only provides us with psychological data, such as, valuable information about the location of gaze, but no information about neural activity. On the other hand, EEG, which measures neuronal activity in humans, does not provide direct information about the eye movements. For this reason, projects that combine EEG and ET in a joint setup have attracted some interest from scientists [75].

Recording precise eye movements together with the EEG is useful for improving ocular artifact correction, controlling fixation, measuring saccadic reaction times, presenting stimuli gaze-contingently, detecting signal distortions from microsaccades and improving brain-computer interfaces [9] [76].

An important aspect of the simultaneous acquisition of eye-tracking and EEG data is the synchronization of the two data streams. The "clock drift" between the two recording computers may cause the time in one recording to not exactly match that in the other. This problem is usually solved by sending common marker signals in both data streams, which can be used to match the data in the analysis phase [77].

Transistor-transistor logic (TTL) is a popular method of integrating equipment in laboratories because of its excellent and reliable timing characteristics. The ET system and the EEG system are configured to send a TTL pulse (a digital signal) at the beginning of each trial or event of interest. The experiment software is configured to receive the TTL pulses from both systems and record the exact time at which the pulse was received. Once the data is recorded, the experimental software can use the timing information of the TTL pulses to match the eye movement data with the EEG data [78].

In addition, the Matlab EEGLAB toolbox [79] is a crucial tool for the analysis and visualization of EEG data, enabling efficient exploration of neural dynamics. The EYE-EEG toolbox is an extension for the open-source Matlab toolbox EEGLAB, which was created in 2012 by Olaf Dimigen and Ulrich Reinacher to allow for integrated studies of electrophysiological and oculomotor data. The toolbox parses, imports, and synchronizes simultaneously recorded ET data and combine it to the EEG as extra channels. Alternatively, EEG data can be aligned to stimulus onsets and analyzed according to oculomotor behavior (e.g. pupil size, microsaccades) in a given trial [47] [76].

Eye movements are imported from the ET raw data or detected with an adaptive velocity-based algorithm and are then added as new time-locking events to EEGLAB's event structure, allowing easy saccade- and fixation-related EEG analysis (e.g., fixation-related potentials). Moreover, based on their correlation with the electrically independent , this toolbox can recognize saccade-related ICA components [9]. Once data has been collected, software such as EEG-LAB and the EYE-EEG can be used to align the data based on the common TTL/Messages.

2.5.4 Modulation of Beta Band Oscillations and Motor Control in Parkinson's Disease

The study of eye movements in PD patients offers unique advantages for quantitative studies of nervous system function, aids in diagnosis, tracks disease progression, and provides insight into the underlying mechanisms of the disease. Additionally, the findings may help researchers develop new therapies or treatments for the disease by targeting the brain regions that control these movements [80].

In the context of movement initiation and motor control, beta band activity (around 13 to 30 Hz) has been found to be relevant. In healthy individuals, beta band activity is observed to decrease just before and during voluntary movement. This decrease is thought to facilitate motor execution by releasing the motor circuits from inhibitory control. However, in PD, there is often an abnormal increase in beta band activity, particularly in the BG. DBS alleviates PD symptoms, possibly by disrupting the abnormal beta synchronization, but their exact relationship is poorly understood [81].

Beta band is typically divided into two subranges: low beta (approximately 13-20 Hz) and high beta (approximately 20-30 Hz). These oscillations are often associated with different cognitive and motor functions. Generally, high beta activity is associated with motor inhibition or the suppression of movement, while low beta activity is linked to motor execution and movement initiation. However, the relationship between beta oscillations and eye movements can vary based on the specific brain regions being stimulated and the timing of the eye movement task [82] [83].

A prominent study in this area was developed in 2013 by Akihiro Yugeta et al [7], who have investigated how beta oscillations in the STN are modulated during visually guided saccade tasks in patients with PD.

The researchers used DBS to record neuronal activity in the STN, while patients performed horizontal prosaccades and antisaccades. The eye movement tasks were indicated by red light-emitting diodes mounted on a blackboard. LFP were recorded from lead contacts in bipolar derivations during the tasks, one to five days after surgery, when leads were externalized and before implantation of the implantable pulse generator. Additionally, EOG and surface electromyography (EMG) were recorded to detect saccade onset and exclude error trials from the analysis, using a Neuroscan software.

The first analysis approach involved a beta-band power spectrum during two specific time intervals: the baseline period (ranging from 1500 to 500 ms before the initiation of a saccade) and the perisaccadic period (spanning from 100 ms before saccade onset to 900 ms after saccade onset) (Figure 2.20). Saccade-related beta-band desynchronizations were observed immediately before and during saccades, suggesting that the reduction of oscillatory beta-band activity in the STN is related to the preparation and execution of saccades. Moreover, the reduction in beta activity was slightly more pronounced in the higher beta frequencies during both prosaccadic and antisaccadic movements.
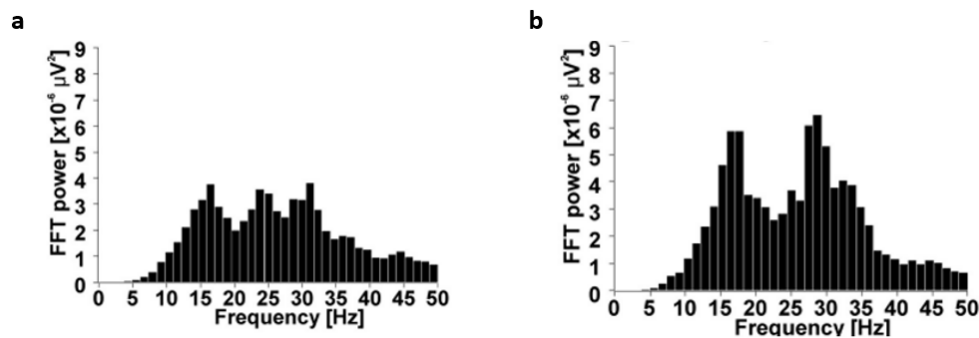
Figure 2.20: Beta-band power spectrums: (a) perisaccade periods and (b) baseline periods during leftward prosaccades. Source: [7].

In addition, to visually evaluate the reduction of beta-band power in the STN related to saccades in both time and frequency domain were created wavelet spectrograms (Figure 2.21). Again, desynchronizations appeared to be more prominent in the high beta range than in the low one.

The results demonstrated that beta-band desynchronizations started earlier, lasted longer, were more pronounced, and were observed more frequently in antisaccades than in prosaccades.

A related 2023 study [84] investigated the impact of plasma levodopa levels, stimulation, and motor performances on the behavior of low- and high-beta peaks in a PD patient undergoing DBS. The evaluation was performed in the following four conditions: OFF medications/ON stimulation, OFF medications/OFF stimulation, ON medications/OFF stimulation, and ON medications/ON stimulation.
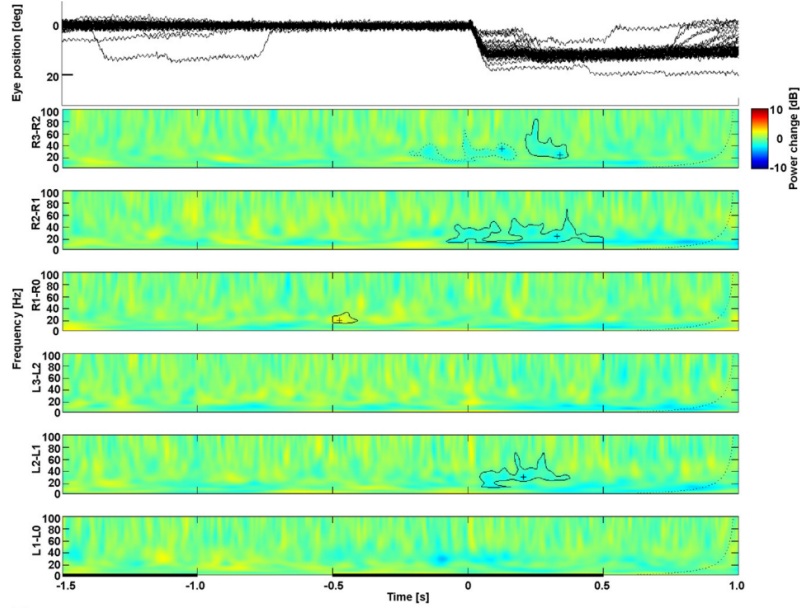
Figure 2.21: Saccade traces and power spectrums during leftward prosaccades. Source: [7].

In the study, PSD estimates were obtained using Welch's method with a 1-second Hamming window, 60% overlap, and a FFT size of 250. Additionally, spectrograms were computed from the resting state LFP time domain signals recorded via the Brainsense™ Streaming feature to compare the signals in each condition. Figure 2.22 displays recordings of left STN LFP in resting state under different conditions. It includes spectrograms, relative spectral power, and highlights low-beta and high-beta peaks.
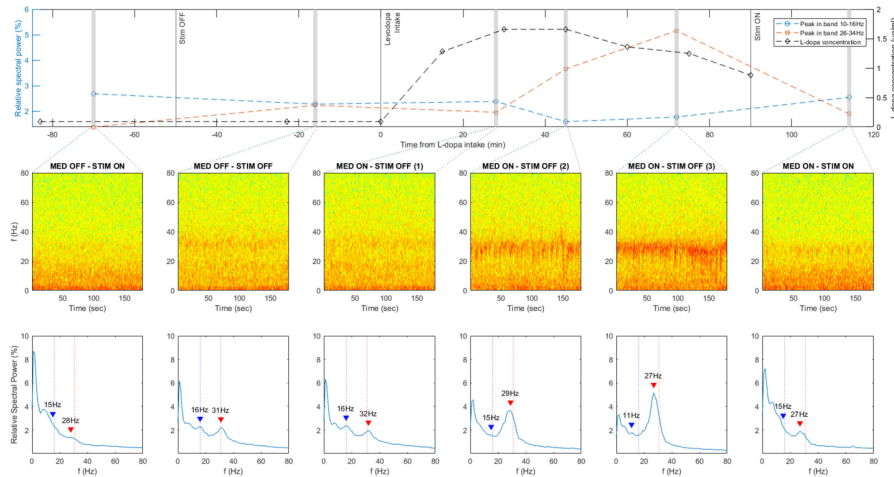
Figure 2.22: Recordings of the left STN LFP in the resting state under different conditions. It includes spectrograms of the raw LFP, the relative spectral power of the beta peaks over time, accompanied by the L-dopa concentration and motor assessments, and highlights the identified low-beta and high-beta peaks. The conditions represented are OFF/ON medications and OFF/ON stimulation. Source: [84].

The results revealed that stimulation suppressed the high-beta peak, while the low-beta peak showed an inconsistent response. Additionally, the high-beta peak correlated with plasma levodopa concentration, exhibiting an incremental amplitude with higher levels. Motor performances were also found to influence the behavior of the beta peaks. These findings emphasize the importance of patient-specific LFP patterns and have implications for personalized closed-loop stimulation in PD treatment. Further research is needed to validate and expand upon these findings.

Furthermore, other studies focused on PD have provided valuable insights into the brain's role in motor symptoms. Explore beta power in the STN and the GPi during rest and movement in PD patients undergoing DBS, showed that GPi exhibited higher beta power and stronger beta desynchronization during movement compared to the STN, with beta power correlating to bradykinesia and rigidity severity [85].

Another study linked event-related beta desynchronization (ERD) in the STN to motor performance in PD patients, revealing potential distinctions in how BG is involved in internally initiated versus externally paced movements. Particularly, the initiation of ERD in the STN occurs before movement initiation, and the timing of ERD is directly connected to reaction time [71].

The scientific articles cited above and the related literature have provided an overview of the current progress in this area. Chapter 3 builds on the concepts already studied to develop a new approach that will continue the research and deepen our knowledge.

3

Methodology

This chapter describes the various steps concerning the development of the proposed methodology for the recording of eye movements-related activity in Parkinson's Disease (PD). Section 3.1, presents how the synchronization between the systems involved in this work was done. Section 3.2, explains the tests performed on a patient and the data acquisition process, followed by a brief description and analysis of the obtained data in Section 3.3. The analytical and statistical techniques employed in the process of data analysis and interpretation is detailed in Section 3.4. Finally, section 3.5, describes the ethical aspects of clinical research required to conduct the study.

3.1 Synchronization Approach

Synchronizing Deep Brain Stimulation (DBS) and Eye Tracking (ET) systems requires careful planning and coordination due to their distinct technologies. The establishment of a specialized configuration becomes imperative in order to facilitate seamless communication between systems. In this study Electroencephalography (EEG) works as a common synchronization element between DBS and ET, being able to receive signals from both.

First, we started by synchronizing ET with EEG . The SR Experiment Builder [86] is an indispensable tool in the field of ET research and analysis, especially when integrating EyeLink data with EEG recordings, since it supports multiple Transistor-transistor logic (TTL) based communication methods. With this software, it is possible to create customized experimental paradigms, define stimulus presentation times and configure triggers for event synchronization.

In the simplest form of TTL integration, a display PC or a stimulating PC, on which Experiment Builder is installed, sends TTL signals that mark critical test events. The TTL signals are simultaneously sent to the EyeLink host PC via an Ethernet cable and to the EEG computer, which is running the System Plus Evolution software (SD Plus amplifier, SystemPlus, Micromed), supported by a BQ USB Express device using a parallel port cable (Figure 3.1).

Based on the protocol used in this work (Section 3.2.1) an Experiment Builder task was constructed so that one TTL is sent when a new movement starts and another when it ends (except for practice tasks). For example, in the fixation task the TTL are sent whenever the center, right, left, up, and down target appears or, in the case of horizontal prosaccades, the TTL
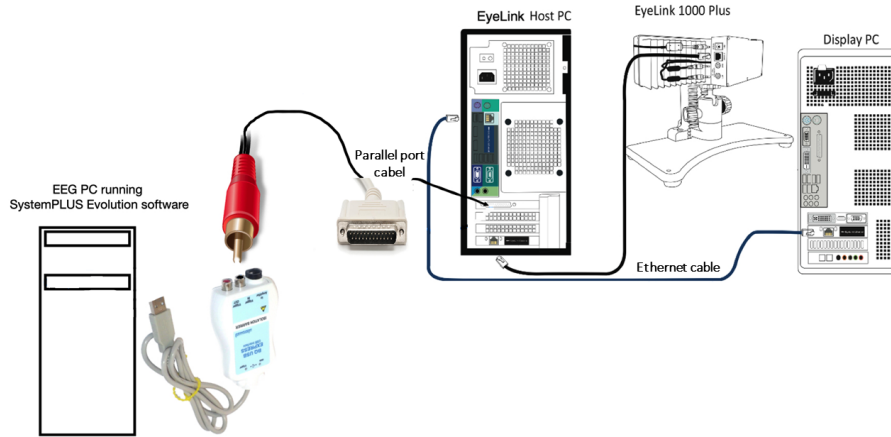
Figure 3.1: System Communication: Integrating EyeLink and EEG Equipment.

is sent whenever the white central fixation point appears and also whenever the blue peripheral targets appear, either on the right or on the left side of the screen.

Each time a TTL is sent to the EEG (with a pulse duration of 10 ms, which was sufficient in an initial experiment for the signal to be detected), a message is marked in the EyeLink data file based on the TTL number. In this way, both data streams have common event markers that can be used to synchronize the time of the data in the analysis phase.

The eye movement recording is measured in milliseconds, while the EEG recording is measured in seconds. This difference in time format may introduce some inaccuracies in synchronizing the two data sources. However, both systems were sampled at high rates: 1000 Hz for the ET data and 1024 Hz for the EEG data. This high sampling rate ensures a temporal resolution of milliseconds and minimizes any loss of data when it is converted all the data to seconds.

Once this was done, we proceeded to the phase of synchronizing the DBS with the EEG. The idea is to create an artifact in the EEG by the on/off of the DBS stimulation, most clearly seen in the amplitude of 1 mA during signal acquisition. These artifacts occurred at the time of the first and the last pulse. At the same time, corresponding amplitude fluctuations were visible in the DBS signal, which served as markers for the first and second triggers. By establishing a temporal relationship between these moments, it is possible to synchronize the two signals and thus precisely define the specific part of interest in the session for analysis.

Therefore, analysis of acquired EEG, eye movements, and local field potentials (LFP) signals includes identification of synchronization markers using time-domain or spectral analysis techniques. Then, resampling and time translation are performed to achieve synchronization between the signal streams, which enables comprehensive and simultaneous analysis of these signals. In the following figure, the synchronization plan is shown schematically in a simple way (Figure 3.2):
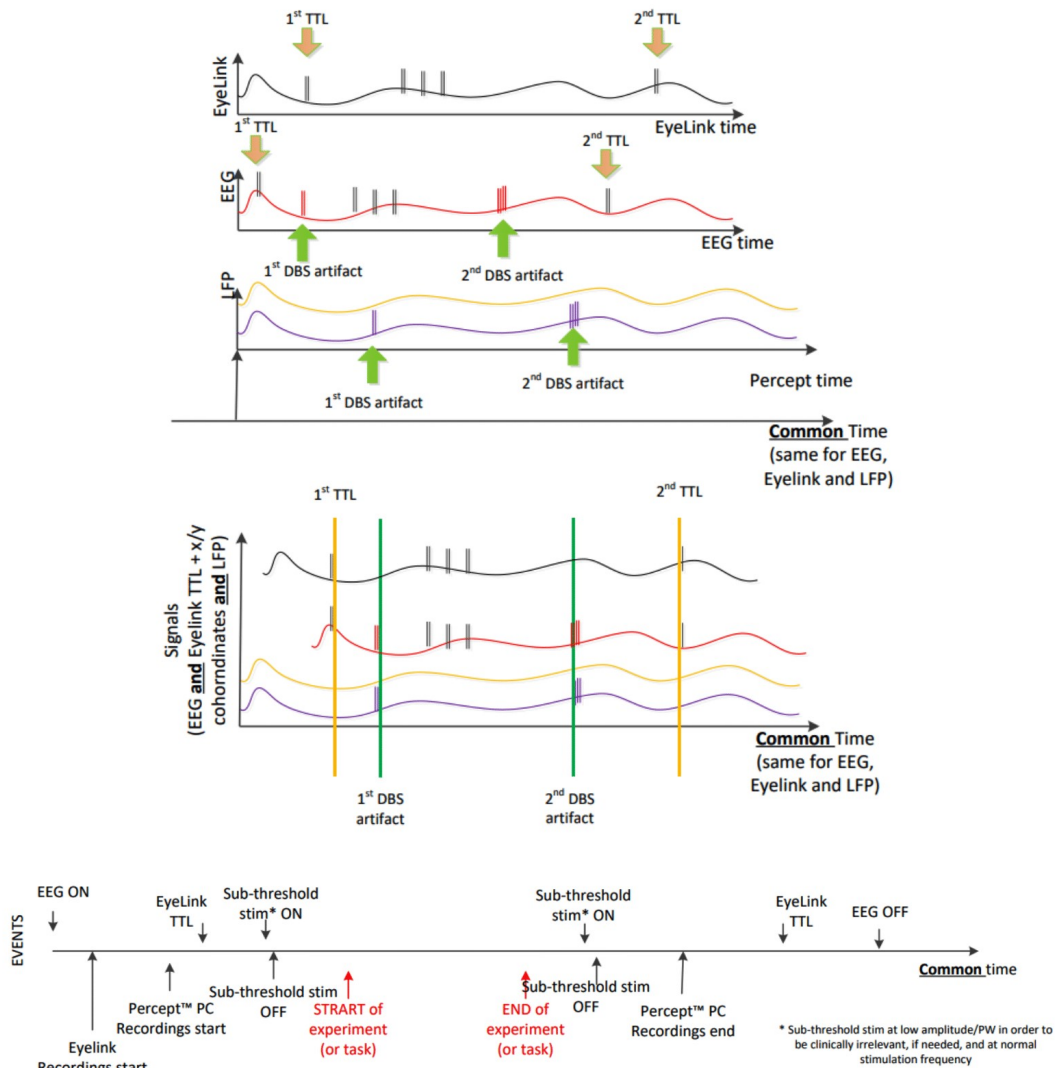
Figure 3.2: Synchronization Concept. Adapted from: [87].

3.2 Data Acquisition Procedure

The study was conducted with a 69-year-old PD male with longstanding PD (27 years) with progressive bradykinesia predominantly affecting the right hemibody. He underwent STN-DBS in 2013 and replacement with Implantable Pulse Generator (IPG)-Percept™ PC in 2017.

During this session, the clinical team, in collaboration with Medtronic, EyeLink and Neuroevolution teams, conducted recordings divided into two parts: with DBS on and with DBS off.

First, the electrodes were placed and EEG recording was started. Using BrainSense™ technology from Percept™ PC, an initial bilateral stimulation of 3 mA was recorded, reduced to 0 mA (one hemisphere at a time), and increased to 1 mA, once streaming began, to mark the artifact in the EEG, and then gradually increased back to the original 3 mA. Once this has been done, the participant was tested in ET by running through all the paradigms (section 3.2.1).

Then, the artifact sent from the DBS to the EEG is repeated to end the session and the EEG is turned off.

The procedure with the DBS off is similar, however it was necessary to consider a waiting time (approximately 1 minute) to gradually turn off the stimulation. Also, in this case, the brain stimulation always remains at 0 mA, keeping only the sending of the two artifacts.

Figure 3.3 represents moments before the acquisition process starts, with the participant already recording EEG signals, getting ready to perform the eye movement tasks.

Figure 3.3: Participant with EEG and Percept™PC performing the eye movements tasks in the EyeLink1000Plus.

3.2.1 Eye Tracking Paradigm

The screen was placed in front of the subject at a 45cm-distance. He was comfortably seated with the head resting and fully stabilized in the tower mount (EyeLink 1000). Eye movement recordings were captured binocularly with a sampling rate of 1000Hz and data from the left eye only was further analysed. The protocol for studying eye movements with the ET system consisted of several tasks (although only prosaccades task was further analyzed, for the purpose of this study):

- Fixation: targets in the center, right, left, top, and bottom are displayed for 10 seconds each. It always starts with the center target and the following targets are then randomly displayed (with respect to the order of their appearance);

- Horizontal and vertical prosaccades: each trial starts with a central fixation point displayed in the center of the screen for 1250-1750ms, which was immediately followed by an eccentric target located 10°to the right, left, up or down, which stood in the screen for 500ms (no gap paradigm);

- Horizontal and vertical prosaccades with variable amplitude: the procedure is similar to the previous case, but the blue peripheral target appears with a variable amplitude (5, 8, 11 and 15°, approximately);

- Horizontal and vertical pursuit: in this task, a blue target is first placed in the center of the screen and then runs sinusoidally from right to left and left to right for a certain number of cycles, and the same from top to bottom and bottom to top in vertical pursuit;

- Horizontal and vertical antisaccades: as in the case of prosaccades, each trial starts with a white central fixation point displayed in the center of the screen for a random time, then it disappears, and immediately a blue 10°peripheral target appears either at the right or left side, or either in the top or bottom of the screen. The difference is that, in this case, the participant must look in the opposite direction of the target.

There are 4 training trials and 64 trials (16 to each side, randomized in order of appearance and latency), for real data acquisition, for each task. This protocol lasts about 30 minutes.

A total of 393 TTL were sent in this session, divided as follows: 5 TTL for fixation (one for each of the positions), 64 TTL for horizontal prosaccades: 16 for the right side, 16 for the left side and 32 for the central target. It is important to notice that at the beginning of the experiment and at the end of each trial an erase pulse must be sent, otherwise the state of the parallel port will not be changed in the following trials and the signal will not be recognized by the EEG.

The same for vertical prosaccades, horizontal and vertical variable amplitude prosaccades and for horizontal and vertical antisaccades. Finally, 2 TTL for horizontal pursuit and 2 TTL for vertical pursuit, one when the pursuit movement starts and another when it ends. This approach is adopted due to the inherent challenge of precisely triggering a TTL signal at the exact moment when smooth pursuit crosses the center or reaches each boundary.

3.3 Data Description and Analysis

During the session, data were collected from three distinct systems, each providing different types of information. The primary objective was to process the collected signals in order to understand the nature of the data received from each device and to identify events that would serve as reference points for the subsequent synchronization.

3.3.1 Percept™PC Data

LFP recordings were performed using BrainSense™ by Percept™PC in Survey and Streaming modes. Preprocessing included applying 100 Hz low-pass and 1 Hz high-pass filters to the raw data. The data was saved in Java Script Object Notation (JSON) files format in the Medtronic Clinician Programmer reports, and imported into Matlab (Mathworks, Natick, MA) with a custom-built code for offline analysis, in which a band-pass filter (10-50 Hz) was used to try to eliminate remaining stimulation and Electrocardiography (ECG) artifacts.

Different studies employ different parameters for DBS stimulation. Table 3.1 highlights the relevant settings considered in this analysis, specifically examined for the right and left hemispheres separately.

Table 3.1: DBS settings for right and left hemisphere.

DBS Settings	Left Hemisphere	Right Hemisphere
Stimulation status	ON	ON
Pulse Width (µs)	60	90
Rate (Hz)	130	130
Frequency (Hz)	25	24
LFP Threshold (mA)	20-30	20-30
Gain (dB)	227	226
Sample Rate (Hz)	250	250
Initial amplitude (mA)	3	3
Average duration (ms)	3000	3000

The first step in preprocessing the Percept™ PC data is to evaluate the Brainsense™ Survey (Section 2.2.1) and understand, in the case of the patient under study, which is the baseline state without stimulation and which contact pair has the highest expression of the beta band, since this is the region from which we expect the greatest benefit and ability to control symptoms with stimulation, for PD. Figure 3.4 shows the 12 possible pairs between the channels of both electrodes:
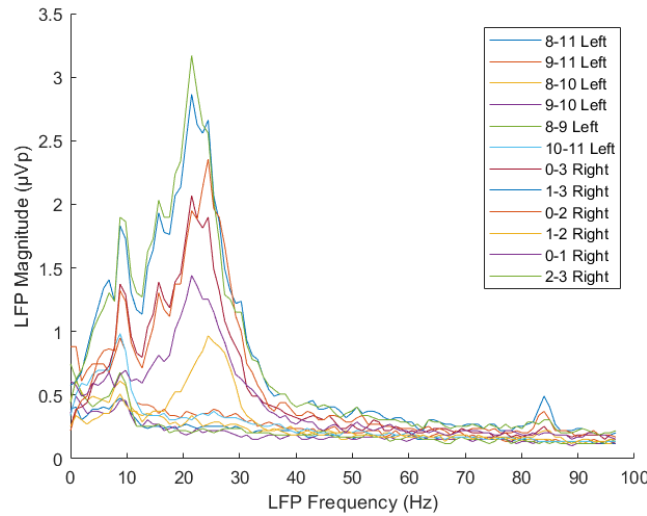
Figure 3.4: Global comparative chart of the 12 possible contact pairs for leads channels.

After analyzing the previous graph, Figure 3.5 (a) shows the choice made for the best pair for the right hemisphere, located between contacts 1 and 3, with a peak magnitude of 2.36 $\mu V p$ and a peak frequency of 24.41 Hz. This means that these are the sites where there is the greatest difference in depth of electrophysiological activity (i.e., one is in a region with much beta band energy and the other in one with much less energy). In the left hemisphere (Figure 3.5 (b)), the best pair is between contacts 9 and 11, with a peak magnitude of 0.46 $\mu V p$ and a peak frequency of about 25 Hz.
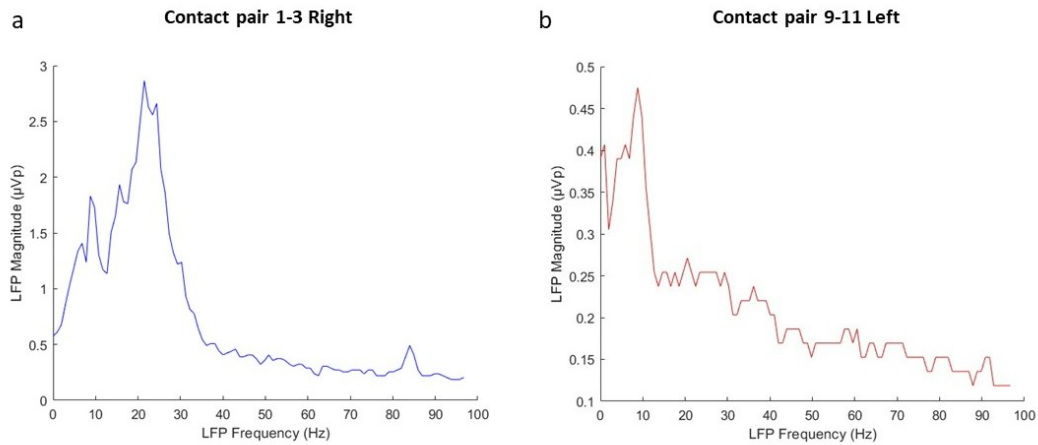
Figure 3.5: Graphical representation of the LFP magnitude variation along the different frequency ranges. The highest beta power was identified between contacts 1 and 3 in the right hemisphere (a) and between contacts 9 and 11 in the left hemisphere (b).

Next, we examined the data from the Brainsense™ Streaming sessions to gain insights into the changes that occurred in the beta band specifically when the patient performed a specific eye movement. Figure 3.6 illustrates the data obtained in the right hemisphere during the on session, as an example.

To achieve synchronization between the LFP recording and the EEG graph, we considered the artifacts identified by the DBS when the stimulation was set at 1 mA, referred to as the first trigger (Figure 3.6 (a)) and the second trigger (Figure 3.6 (b)).
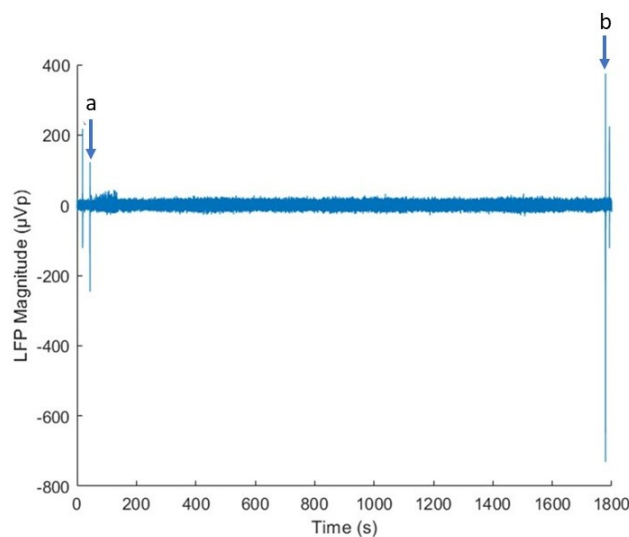
Figure 3.6: Analysis of BrainSense™ Streaming session data over time in the right hemisphere with DBS on. Arrows (a) and (b) denote the first and second triggers, respectively, marking the region of interest within the graph.

In both hemispheres, the DBS on triggers were marked at 45 seconds and at 1779 seconds. On the other hand, for the DBS off, the first trigger occurred at 29 seconds, and the second trigger was observed at 1774 seconds, also in both hemispheres.

3.3.2 EyeLink Data

Preliminary ET results showed that eye recordings have good quality and can be used for analysis, except for antisaccades, which were poorly performed and highly prone to artifacts, both in on and off sessions. Horizontal pursuit eye movements also occasionally showed artifacts in on session, as well as, the right eye's vertical pursuit movement in off session. Futhermore, vertical prosaccades were more unpredictable compared to horizontal prosaccades, with varying amplitudes.

Eye movement data obtained from EyeLink is typically stored in an Eyelink Data Format (EDF) file. Raw data was firstly analysed in Experiment Builder and then extracted, filtered, and analysed using DEMoNS Protocol algorithms [62] [63].

An initial analysis was performed on the data collected from each of the eye movement tasks in both the DBS on and off sessions and for both eyes, to ensure that the test had been performed correctly.

To clean the raw signal from eye position, a second-order low-pass filter with a cut-off frequency set at 10% of the sampling frequency was applied. In addition, a nine-sample smoothing kernel was used to further reduce noise and prepare the signal for velocity estimation [62].

An example plot obtained from the analysis, specifically for horizontal prosaccades with the device turned on, is illustrated in Figure 3.7. In the provided graph, the black line represents the target, while the red and blue lines represents the gaze position of the left and right eye, respectively. The similarity of the paths among all the three lines indicates the quality of the test performance suggesting a more accurate and precise test result.
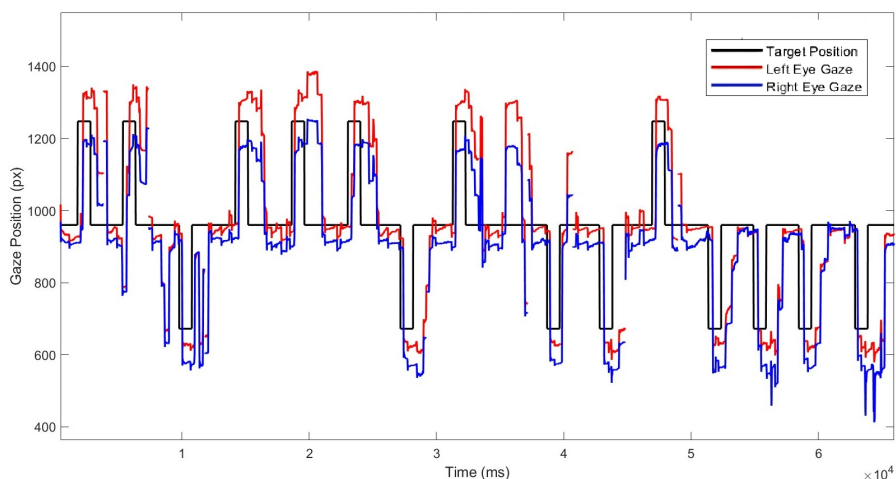
Figure 3.7: Part of the Horizontal Prosaccades task performed by the participant for both eyes with DBS on.

Figure 3.8 demonstrates the repetition of the identical task while deactivating the implanted device. As expected, the test performance is better when the DBS is switched on.
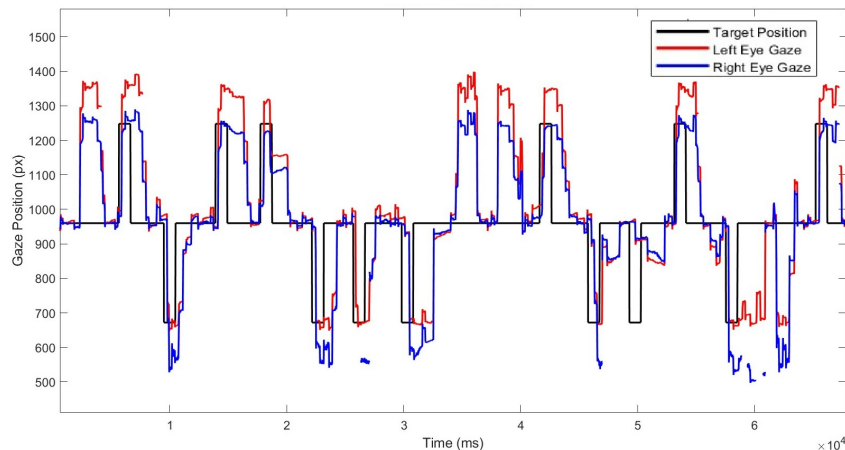
Figure 3.8: Part of the Horizontal Prosaccades task performed by the participant for both eyes with DBS off.

In the same files, we also have access to messages marking the TTL during each task. This helps precisely match the timing with the EEG data, making it easier to analyze and find correlations between them. Table 3.2 and Table 3.3 display the synchronization marks for ET tasks, showcasing the TTL values and corresponding timing at the start and end of each task with DBS on and DBS off, respectively.

Table 3.2: EyeLink TTL values and corresponding timing at the start and end of each task with DBS on. The numbers represent different ET tasks as follows: fixation (1), horizontal prosaccades (2), vertical prosaccades (3), horizontal prosaccades with variable amplitude (4), vertical prosaccades with variable amplitude (5), horizontal pursuit (6), vertical pursuit (7), horizontal antisaccades (8) and vertical antisaccades (9).

ET Task	1	2	3	4	5	6	7	8	9
Start	TTL1 0.092s	TTL6 0.096s	TTL70 0.092s	TTL134 0.102s	TTL198 0.101s	TTL262 1.092s	TTL264 1.090s	TTL266 0.094s	TTL330 0.095s
End	TTL5 40s	TTL69 125s	TTL133 125s	TTL197 125s	TTL261 125s	TTL263 41s	TTL265 51s	TTL329 135s	TTL393 125s

Table 3.3: EyeLink TTL values and corresponding timing at the start and end of each task with DBS OFF. The numbers represent respectively the different ET tasks.

ET Task	1	2	3	4	5	6	7	8	9
Start	TTL1 0.095s	TTL6 0.093s	TTL70 0.095s	TTL134 0.091s	TTL198 0.096s	TTL262 1.092s	TTL264 1.099s	TTL266 0.093s	TTL330 0.091s
End	TTL5 40s	TTL69 125s	TTL133 125s	TTL197 125s	TTL261 125s	TTL263 41s	TTL265 51s	TTL329 135s	TTL393 125s

It is important to note that the exact durations of all TTL in each task were carefully considered and played a crucial role in the analysis, although only the first and last values are presented in the previous tables.

3.3.3 Electroencephalography Data

EEG recordings were obtained using scalp gold-plated disc electrodes arranged in a monopolar assembly with 31 lines, following the international 10-20 system. The setup included 27 EEG channels and 3 bipolar channels (EOGd, EOGe, ECG), along with an extra channel for receiving triggers (MKR). G2 served as the reference electrode, while G1 was used as the ground electrode.

The EEG signals were acquired using an SD Plus amplifier from Micromed, with a sampling frequency of 1024 Hz. To ensure accurate recordings, a low-pass filter at 276 Hz and a high-pass filter at 0.15 Hz were applied during the data acquisition process. The clinical EEG software was used for reviewing the EEG tracings, which were displayed in both bipolar and referential montages.

To visualize the recorded EEG data, an EEG viewer program was used. This tool allows for the visualization of the entire recorded signal in each channel for both the DBS on and off sessions.

Figure 3.9 showcases a segment of the recorded signal from the session with the device turned on. It includes annotations made by the technicians, such as the label 'first trigger' which indicates a notable event or stimulus identified during the recording, in this case the first artifact sent by the DBS device. In the bottom of the figure, there is also, highlighted with a red circle, a typical example of the EEG marks generated by the TTL signals sent from the ET device.
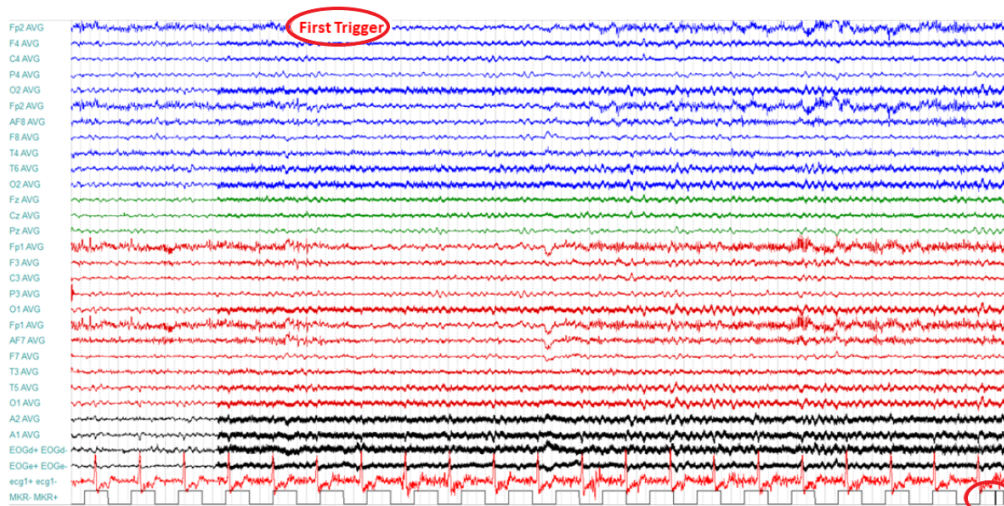
Figure 3.9: An illustrative segment of the recorded EEG signal during a session with DBS on.

The EEG data were stored in an European Data Format (EDF) file format, to perform initial analysis and signal processing, in Matlab. Various signal processing techniques were applied, including filtering. In this case, a cutoff frequency of 10 Hz was used during the signal processing stage.

Figure 3.10 shows a portion of the processed EEG signal from channel Fp1. The EEG channel highlighted in the figure was randomly selected, because it is used only for synchronization and is not relevant to the analysis. To focus our analysis, we selected a time interval starting from the first trigger (298 seconds) marked by the DBS signal on the EEG, and extending to the time of the second trigger (2081 seconds) in this case of the session with DBS on.

For the off session, the first DBS trigger on the EEG was considered at 308 seconds and the second at 1547 seconds. This time interval was chosen as our area of focus, relevant to examine the dynamics of the beta band during eye movements when the patient was not being stimulated.
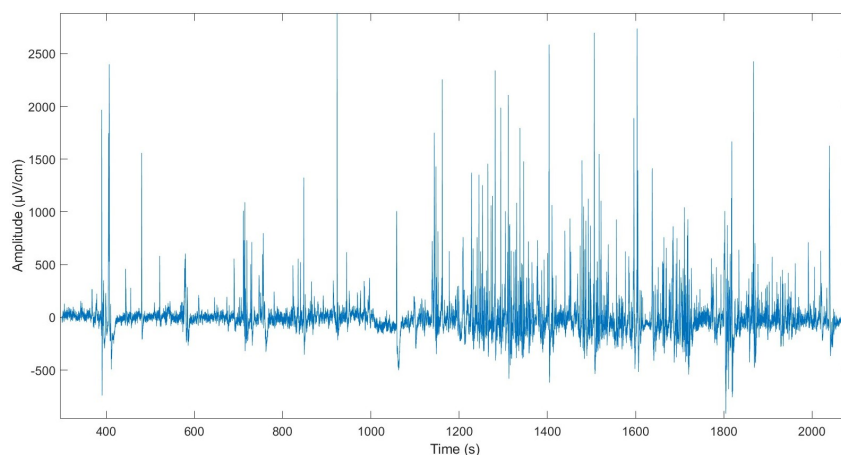
Figure 3.10: Processed EEG signal from channel Fp1 in the session with DBS on.

In order to isolate the EEG data corresponding to each ET task, we needed to identify the TTL marks recorded in the EEG. The timestamps for these TTL signal can be found in Table 3.4 and Table 3.5.

Table 3.4: EEG marks from EyeLink device transmitted TTL: Start and End times of each task during session with DBS activated. The numbers represent different ET tasks as follows: fixation (1), horizontal prosaccades (2), vertical prosaccades (3), horizontal prosaccades with variable amplitude (4), vertical prosaccades with variable amplitude (5), horizontal pursuit (6), vertical pursuit (7), horizontal antisaccades (8) and vertical antisaccades (9).

ET Task	1	2	3	4	5	6	7	8	9
Start	738s	817s	983s	1152s	1317s	1046s	1106s	1703s	1884s
End	778s	967s	1133s	1304s	1469s	1074s	1125s	1849s	2034s
Duration	50s	150s	150s	152s	152s	38s	38s	146s	146s

Table 3.5: EEG marks from EyeLink device transmitted TTL: Start and End times of each task during session with DBS deactivated. The numbers represent different ET tasks as follows: fixation (1), horizontal prosaccades (2), vertical prosaccades (3), horizontal prosaccades with variable amplitude (4), vertical prosaccades with variable amplitude (5), horizontal pursuit (6), vertical pursuit (7), horizontal antisaccades (8) and vertical antisaccades (9).

ET Task	1	2	3	4	5	6	7	8	9
Start	325s	400s	560s	712s	862s	1046s	1106s	1179s	1352s
End	475s	551s	711s	856s	1025s	1074s	1125s	1326s	1499s
Duration	50s	151s	151s	144s	163s	28s	19s	147s	147s

By following this approach, we acquired the processed and treated signals of interest, along with their synchronization marks, which are fundamental for subsequent data analysis and interpretation.

3.4 Statistical Analysis

Data were described using the mean ± 2 standard deviations. Saccades were compared according to direction both in DBS on and off periods, using Kruskal Wallis procedure, followed by post-hoc analysis (Mann Whitney procedure) if significance was observed.

Comparisons between saccades during DBS on and off were performed using Wilcoxon procedure. Interaction analysis was performed using two way ANOVA (Analysis of variance) procedure using DBS status (on vs. off) as within-group factor and saccade direction (rightward vs. leftward) as between-group factor. A similar approach was used to investigate vertical saccades.

Beta band potency in right and left hemispheres and both during DBS on and off periods, related to rightward saccades, leftward saccades and baseline periods, was compared using Kruskal Wallis procedure, followed by post-hoc analysis (Mann Whitney procedure) if significance was observed. If no significance was demonstrated, Mann Whitney procedure between the baseline period and one saccade direction period, or between two saccade directions periods was still applied. The latter approach was important to further investigate the possibility of a directional saccadic bias in each hemisphere, i.e., differences in brain activity during rightward vs. leftward saccade periods.

An additional index was created to investigate directional saccadic bias in one hemisphere, as demonstrated in Equation 3.1:

$$\frac{\text{beta band potency ipsilateral hemisphere} - \text{beta band potency contralateral hemisphere}}{\text{beta band potency ipsilateral hemisphere} + \text{beta band potency contralateral hemisphere}} \tag{3.1}$$

Comparisons between saccade-related beta band potency during DBS on and off were performed using Wilcoxon procedure. Interaction analysis was performed using two way ANOVA

procedure using DBS status (on vs off) as within-group factor and saccade direction (rightward vs. leftward) as between-group factor. A similar approach was used to investigate vertical saccades and also beta band potency analysis to investigate mean LFP amplitude.

Correlation analysis between brain data (beta band potency, LFP amplitude) and saccade data was performed using Spearman procedure. Furthermore, SPSS version 20 was used for the analysis. A p value < 0.05 was considered significant.

3.5   Ethical Approval

A submission of the project study has been sent to the Medical Ethics Committee of the Centro Hospitalar e Universitário de Coimbra (CHUC). The patient gave written informed consent.

4

Results

This chapter presents the results obtained in the present work, along with their interpretative analysis and discussion. Section 4.1 shows the results of the synchronization of Deep Brain Stimulation (DBS) with Eye Tracking (ET). Section 4.2 presents the findings from the analytical, visual and statistical analysis related to saccadic metrics, beta band potency, and LFP amplitude.

4.1 Synchronization Between Systems

In order to accomplish the main goal of this work, the key step is to synchronize the DBS and ET tracings, using the Electroencephalography (EEG) tracing as a reference. With this synchronization, it is possible to monitor and analyze the brain's response precisely when the participant performed a specified eye movement. To achieve this, we followed the methods outlined in Chapter 3.

As a result, we successfully obtained a graph representing the three systems synchronized in time. Figure 4.1 shows the entire horizontal prosaccades task during the session with DBS on. The first graph displays the local field potentials (LFP) magnitude over time in the right hemisphere. The second graph represents the EEG signal's amplitude specifically from the Fp1 channel (used as a representative example) over time. The third graph illustrates the left gaze position over time, while performing left and right saccades. All with the same time axis.

After successfully synchronizing one example, it becomes feasible to replicate the process for other cases while considering the corresponding synchronization marks of the three systems involved. In addition, we have the flexibility to select any time interval of a specific task for analysis, along with the corresponding signals from DBS and EEG.

The investigation of eye movements is a highly intricate field, and there remains a vast amount to uncover, as studied in Section 2.3. To address this issue, our initial approach involved comparing patterns of LFP activity between the two hemispheres of the brain. This comparison may provide valuable information about the neuronal mechanisms underlying eye movements and their potential lateralization effects, thus contributing to the overall understanding of the brain's role in eye movement coordination.
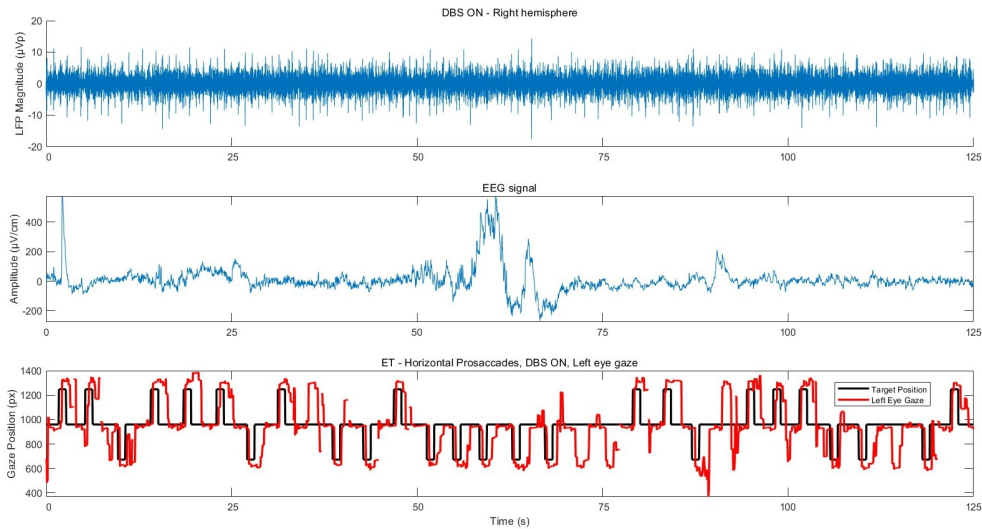
Figure 4.1: Temporal synchronization of the three systems under study. This demonstrative example focuses on the right hemisphere data obtained during the DBS on session, specifically for analyzing left eye gaze during horizontal prosaccades.

As an example, Figure 4.2 shows 8 seconds of the DBS on session capturing the occurrence of two rightward saccades and the respective LFP signals from both right and left hemispheres.
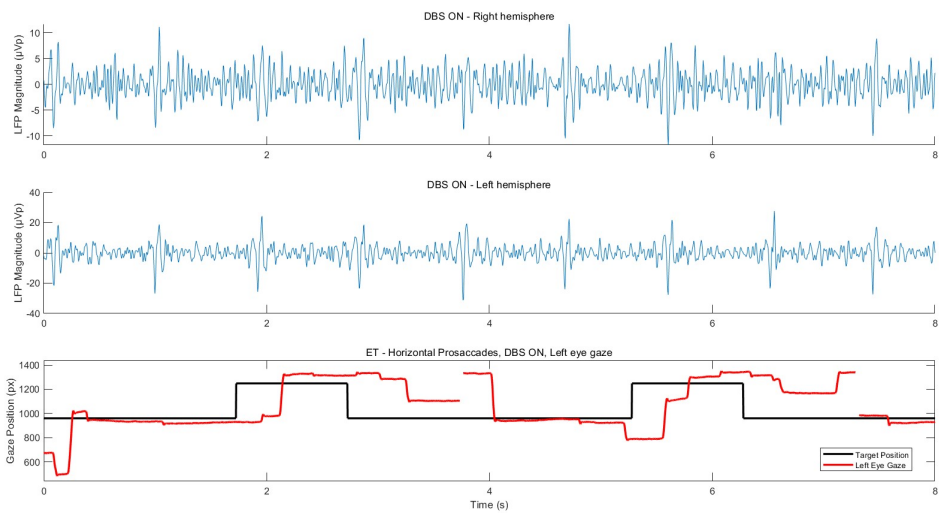
Figure 4.2: Synchronized LFP data obtained from both hemispheres in the session with DBS turned on. The focus of the analysis is on the left eye gaze during horizontal prosaccades.

On the other hand, Figure 4.3 presents a distinct example featuring a portion of 2 second duration of the signals. The figure visually captures a vertical downward saccade along with the corresponding brain activity in both hemispheres when the participant executed this particular eye movement.
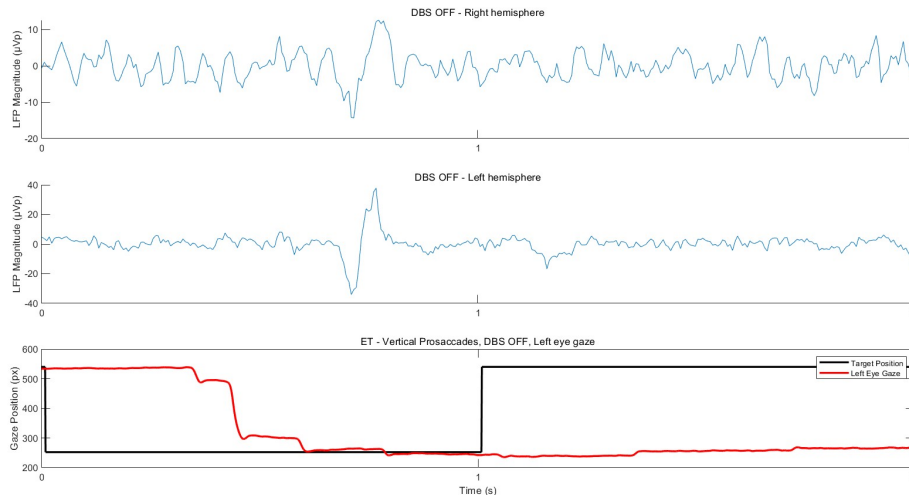
Figure 4.3: DBS off session, specifically for analyzing LFP activity in both hemispheres during left eye gaze in vertical prosaccades.

4.2 Statistical and Visual Results

After achieving the temporal synchronization of DBS and ET systems, visual and statistical analysis of possible clinical outcomes were initiated.

The study was centered around analyzing horizontal and vertical prosaccades, both under conditions of DBS activation and deactivation. Furthermore, the investigation targeted two main temporal segments: The perisaccadic period which denotes the temporal window surrounding the initiation of saccades, including the activity during and just after the movement, and the baseline period which refers to the timeframe preceding the saccadic movement, when the participant is in a resting state, fixating on the central target.

The time intervals of interest were defined by the temporal marks in both systems. However, in order to maximize the analysis accuracy, only the initial 0.5 seconds of each perisaccadic period and the final 0.5 seconds of each baseline period were taken into consideration, due to some errors in the participant's performance, such as involuntary saccades occurring during intended fixation between stimuli.

Figure 4.4 showcases the 16 rightward, leftward, upward and downward saccades performed by the participant within each session. The color blue indicates the on session, while the color red represents the off session. An initial visual examination reveals the increase of amplitude of leftward saccades and the decrease of latency of downward saccades when DBS is on.

To complement, the baseline period between horizontal and vertical saccades reveals its characteristics in Figure 4.5. Although a few seconds were omitted from the recording, it is still evident that the participant's pathological condition hinders the achievement of a perfect fixation during these intervals.
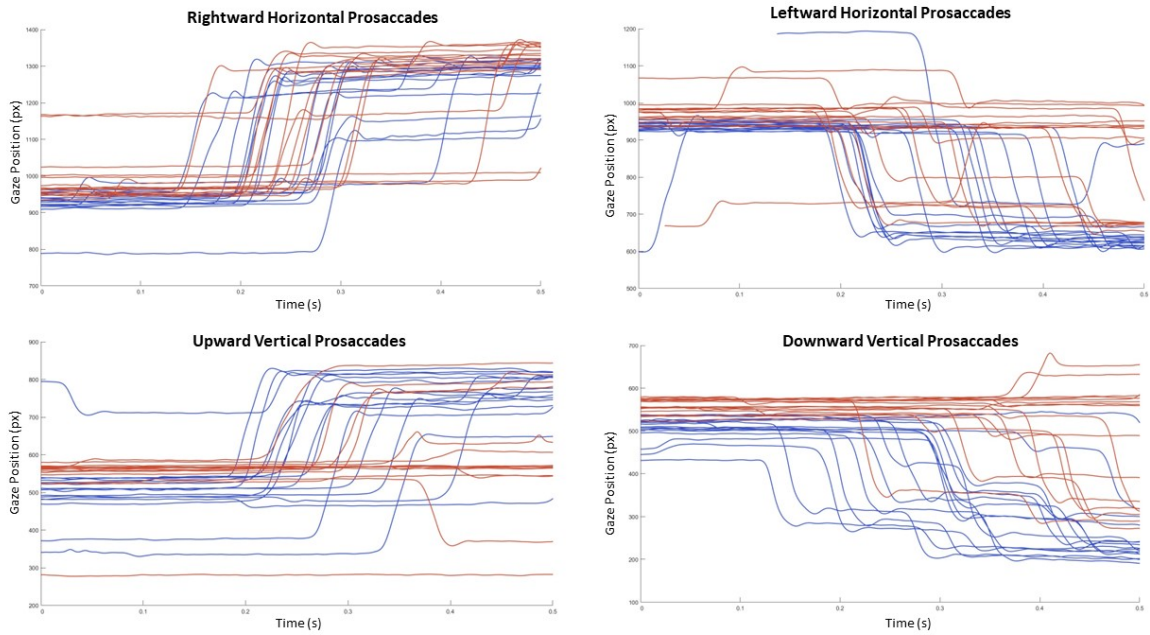
Figure 4.4: Saccadic eye movement recordings (blue, DBS on; red, DBS off).
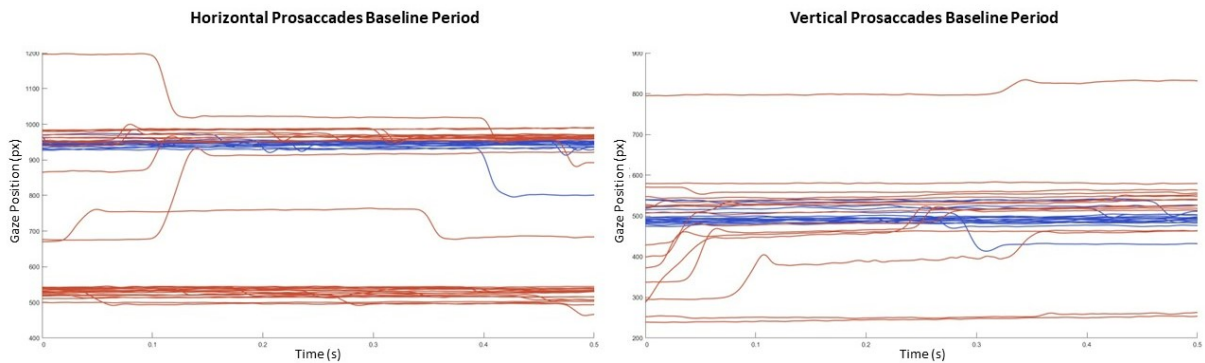
Figure 4.5: Baseline period eye movement recordings (blue, DBS on; red, DBS off).

4.2.1 Saccades

First, in the context of this study, different metrics related to eye movements were calculated and evaluated using ET technology, including latency, peak velocity, and gain. The data were collected during horizontal and vertical prosaccades, both with and without the application of DBS.

The calculated values for each time segment are presented individually, alongside respective averages and pattern standard deviations in Table A.1 for horizontal prosaccades and in Table A.2 for vertical prosaccades.

With DBS off, latency of downward saccades (497±168) was significantly higher than the latency of rightward saccades (245±80.4) (p=0.013). Similarly, velocity of downward saccades (330±58.5) was significantly lower than the velocity of rightward saccades (420±96.4) (p=0.013).

With DBS on, the velocity of vertical saccades (upward (326±65.2) and downward (278±79.2)) was significantly lower than the velocity of horizontal saccades (rightward (473±64.8) and leftward (459±36.6)) (p=0.000). Additionally, the gain of downward (0.58) saccades was significantly lower than gain for all other directions (p=0.000).

When comparing DBS off vs. DBS on, the gain of leftward saccades significantly increased with DBS on (0.99±0.05) when compared with DBS off (0.86±14) (p=0.018). The latency of upward saccades was significantly shortened with DBS on (236±72.8) when compared with DBS off (405±151) (p=0.035). Similarly, the latency of downward saccades was significantly shortened with DBS on (275±112) when compared with DBS off (497±168) (p=0.000).

There were no significant interactions between saccade direction and DBS status.

In sum, the velocity and/or gain of vertical (downward and/or upward) saccades was lower than that of horizontal saccades. With DBS on, a clear effect on saccade performance was seen, i.e., the gain of leftward saccades was increased and the latency of vertical saccades was shortened (Figures 4.6, 4.7 and 4.8 shows the correspondent box-plots of saccadic velocity, gain and latency, supporting the previous statements).
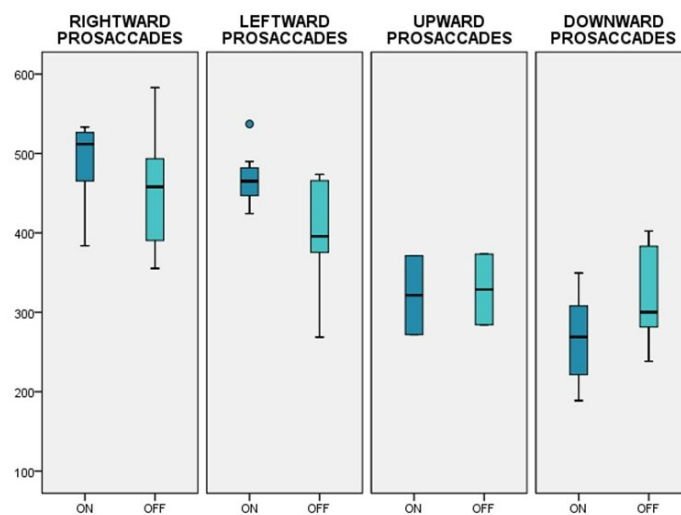
Figure 4.6: Box-plot of saccadic velocity.
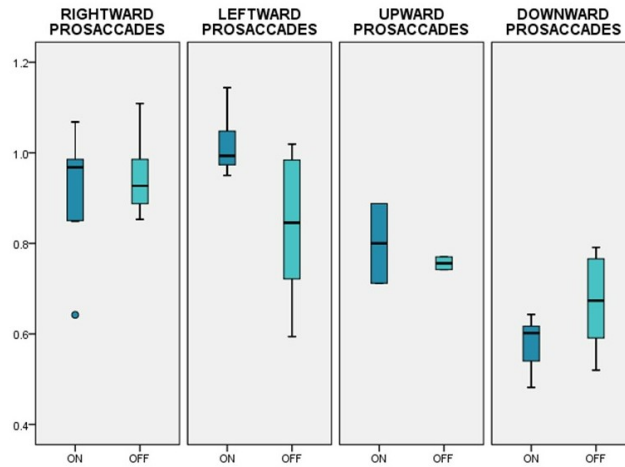
Figure 4.7: Box-plot of saccadic gain.
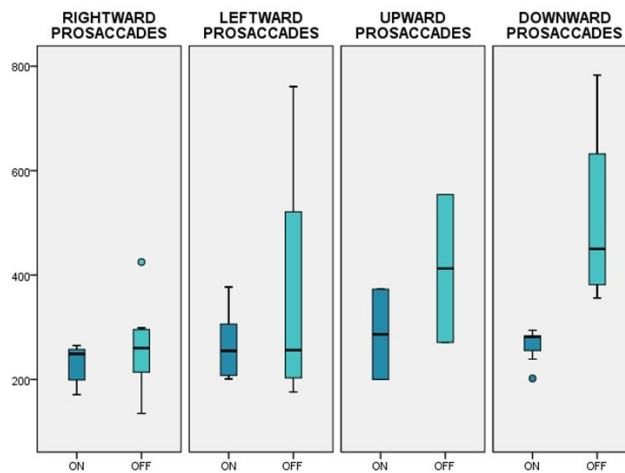
Figure 4.8: Box-plot of saccadic latency.

4.2.2 Beta Band Potency

Beta band oscillations have been implicated in the motor symptoms of Parkinson's Disease (PD). Previous studies have indicated that increased beta band activity is associated with these symptoms and have demonstrated that beta-band desynchronization in the subthalamic nucleus (STN) is reduced in the execution of movements [7] [84]. Based on this, we hypothesized the study of beta band potency variation during saccade tasks, to evaluate the behavior of the brain and try to meet the expectations of the literature and deepen the knowledge in this area.

The power spectrum analysis provides insights into the distribution of power across various frequencies within the beta band. It offers information about the primary frequencies in the beta range and their relative contributions to the total beta power observed in the STN.

As in previous studies, the reduction in beta power during prosaccades appeared to be slightly greater in the high-beta (20–30 Hz) than in the low-beta (15–19 Hz) band, providing more substantial data insights in the higher frequencies. Consequently, we started by considering only the beta band frequencies between 25 and 30Hz.

Figure 4.9 and Figure 4.10 demonstrates the baseline and perisaccade beta band power spectra, during rightward and leftward prosaccades with DBS on and off, respectively. These graphs were also replicated for the vertical prosaccades in both sessions
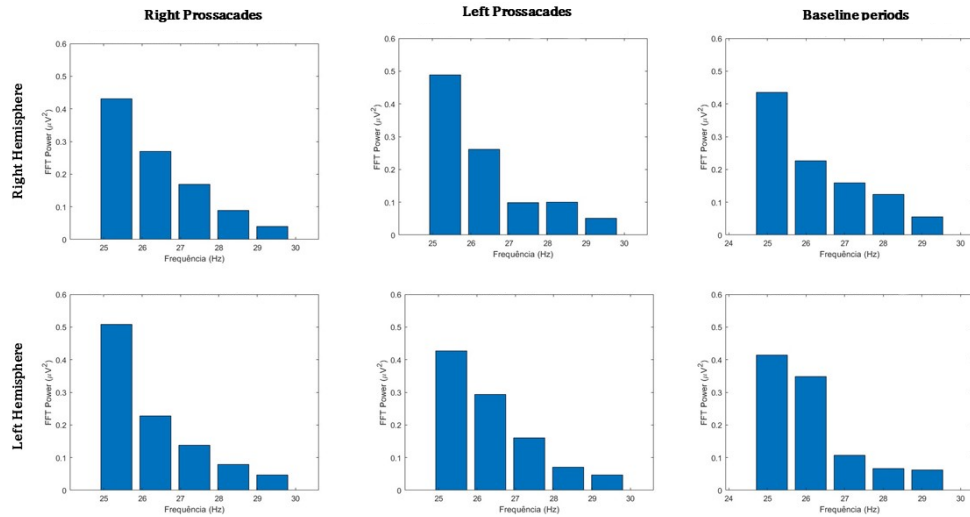
Figure 4.9: Baseline and perisaccade beta band power spectrum during rightward and leftward prosaccades with DBS on.
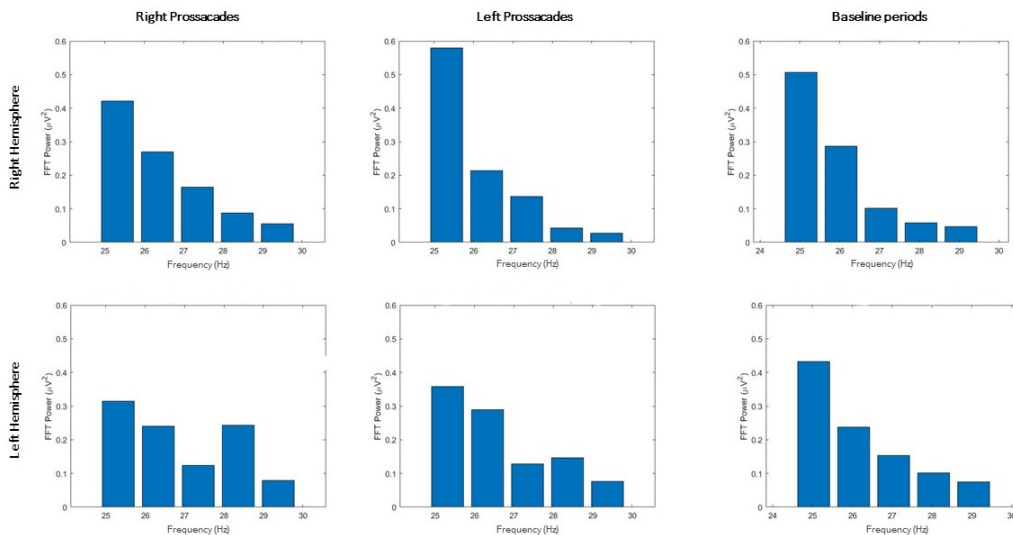
Figure 4.10: Baseline and perisaccade beta band power spectrum during rightward and leftward prosaccades with DBS off.

Visually, it can be seen that a stronger variation in beta power was observed during the baseline period. Moreover, a contralateral control mechanism seems to be detected when com-

paring the two hemispheres, which suggests that the hemisphere opposite to the side of the movement takes a crucial role in orchestrating that movement. For example, when the participant performed leftward prosaccades with DBS turned off, a reduction in beta-band activity was observed in the right hemisphere compared to the left hemisphere.

So far, we only used streaming data from DBS to achieve temporal synchronization. By creating a spectrogram, we can represent the LFP data with respect to both time and frequency domains, which allows to observe variations and patterns in the beta waves.

Figure 4.11 shows an averaged power spectrogram obtained from 16 rightward, 16 leftward prosaccades and the first 16 baseline periods. Blue represents desynchronization and yellow represents synchronization of LFP, which appeared to be more prominent in the beta band specifically in high-beta band. When we contrast the baseline period with the perisaccadic period, there appears to be a noticeably higher level of intensity in the beta band power during the intervals that occur between saccades. Apart from the mentioned observation, it was challenging to deduce any further conclusions from this graph based solely on visual analysis.
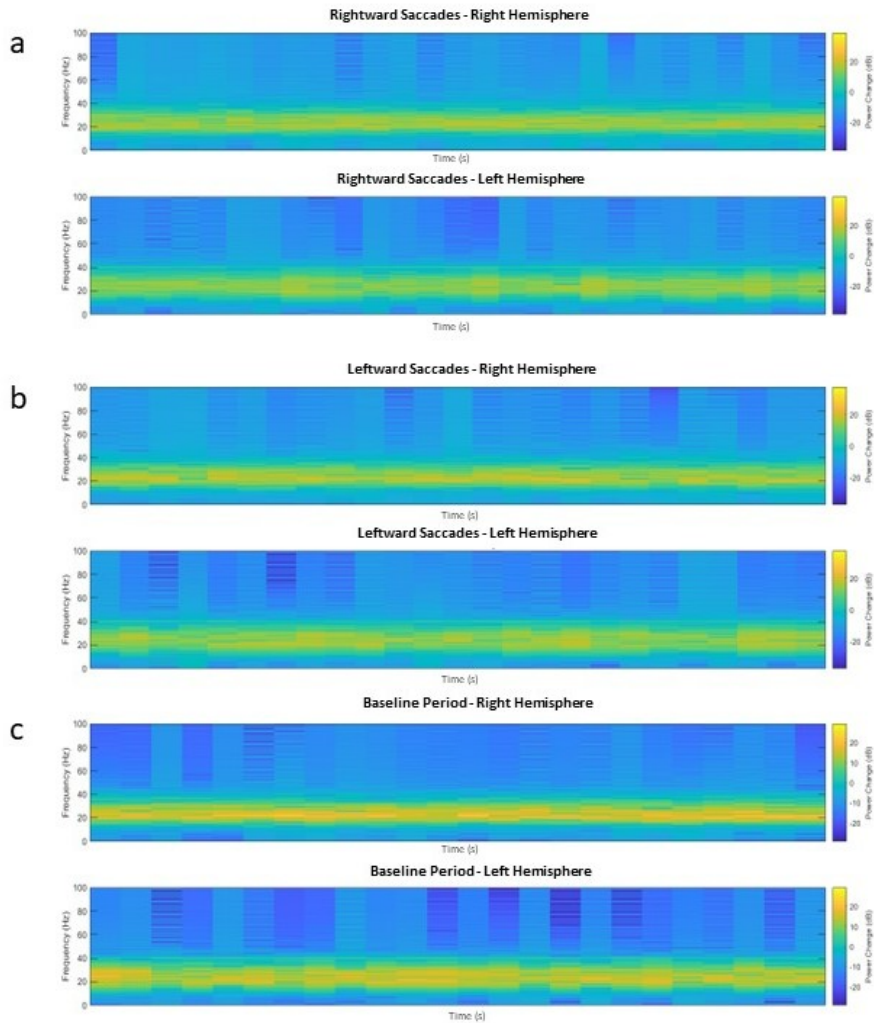
Figure 4.11: Average power spectrograms of horizontal perisaccade and baseline periods in session with DBS off.

Based on the bar graphs (like the example in the Figure 4.9) we decided to calculate the area under the curve for the different types of movements, 16 saccades to the right/up, 16 saccades to the left/down, and the first 16 baseline periods. We did this both with and without DBS active, for both the left and right hemispheres. We also compared the values of the two frequency ranges in the beta band: 20-30 Hz and 25-30 Hz. The results are presented in Table A.3 and Table A.4 for horizontal prosaccades and Table A.5 and Table A.6 for vertical prosaccades. These were the values used for the statistical tests.

In addition to the previous visual examination, the statistical findings indicated that there were no significant differences in beta band potency between the baseline period and horizontal saccades execution period, either with DBS off or on. However, when looking for potential asymmetries between rightward and leftward saccades in each hemisphere's beta band potency, we found that while DBS was off, the right hemisphere beta band potency was near-significantly lower during leftward saccades when compared with rightward saccades (0.77 ± 0.12 vs. 0.70 ± 0.13; p=0.056).

Additionally, if using a weighted index, right hemisphere beta band weighted potency was indeed significantly lower than left hemisphere beta band weighted potency during leftward saccades (p=0.044). We could not find a similar pattern in the left hemisphere, i.e., lower beta band potency during rightward saccades when compared with leftward saccades.

Furthermore, right hemisphere beta band potency during leftward saccades was significantly lower than left hemisphere beta band potency during rightward saccades (0.70 ± 0.13 vs. 0.79 ± 0.07; p=0.012) with DBS off. Importantly, when DBS was on, left hemisphere beta band potency during rightward saccades could be significantly decreased when compared to DBS off (0.72 ± 0.11 vs. 0.81 ± 0.07; p=0.034) (Figure 4.12).
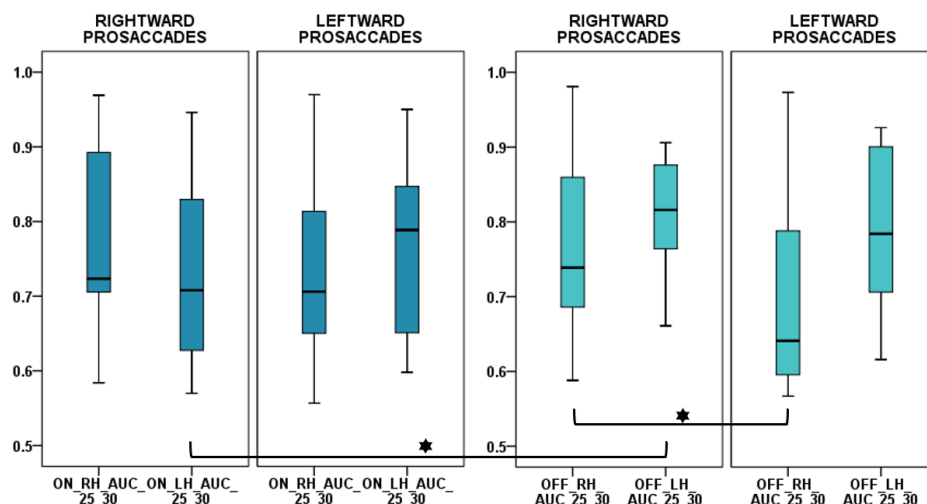
Figure 4.12: Box-plots of beta band potency in the right and left hemisphere during the execution of horizontal saccades. Significant differences are marked with an asterisk.

Finally, right hemisphere beta band potency showed a significant interaction between DBS status (on vs. off) and saccade direction (rightward vs. leftward) (F=6.603; p=0.013), i.e., beta band potency decreased during leftward saccades while simultaneously increasing during rightward saccades, when DBS was on (Figure 4.13).
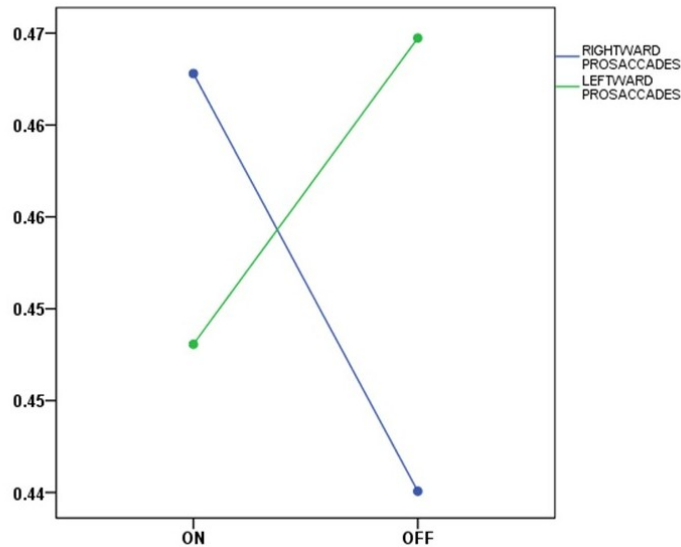
Figure 4.13: Interaction-plot between right hemisphere beta band potency (Y axis) and DBS status (X axis).

Concerning vertical saccades, left hemisphere beta band potency was significantly lower during vertical saccades than baseline (0.71±0.12 vs 0.78± 0.12; p=0.022), with DBS on. There were no significant asymmetries between upward and downward saccades in either hemisphere during DBS on or off and there were no significant interaction between DBS status (on vs. off) and saccade direction (upward vs. downward) either.

Also, there were no significant differences in beta band potency in either hemisphere with DBS on or off, during execution of horizontal vs. vertical saccades.

Left hemisphere beta band potency positively correlated with the gain of horizontal saccades (R=0.58; p=0.002) and rightward saccades (R=0.67; p=0.016) with DBS on, and with velocity of vertical saccades (R=0.52, p=0.039) with DBS off. Right hemisphere beta band potency positively correlated with the gain of upward saccades (R=0.88; p=0.019) with DBS off (Figure 4.14).

In sum, while DBS was off, the right hemisphere (but not the left) showed a pattern of activation where beta band potency was decreased specifically during the execution of contralateral (leftward saccades). Importantly, with DBS on, such pattern was "restored" in the left hemisphere, i.e., decrease of beta band potency during the execution of contralateral (rightward) saccades, as consistently shown in association, interaction, and correlation analysis.
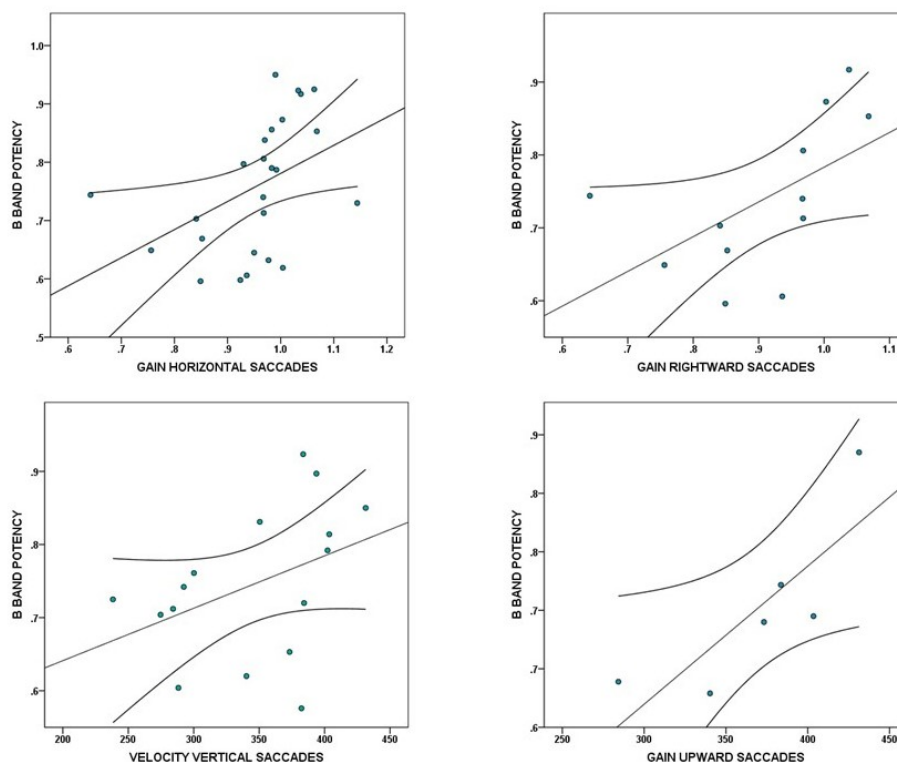
Figure 4.14: Correlation-plots between beta band potency of the left hemisphere with DBS on (top) and off (bottom left), beta band potency of the right hemisphere with DBS off (bottom right), and saccade parameters.

Vertical saccades-related beta band potency changes did not demonstrate such directional bias, but, unlike horizontal saccades, where associated with a global decrease of beta band potency when compared to their baseline period (fixation).

4.2.3 Local Field Potentials Amplitude

Lastly, an analysis was made of the variation in LFP amplitude over time, which can aid in identifying general alterations in neuronal activity during eye movements. To accomplish this, the mean LFP amplitude was calculated within each time interval. The obtained values for horizontal prosaccades are shown in Table A.7 and Table A.8 and for and vertical in Table A.9 and Table A.10, respectively.

Statistically, there were no significant differences between rightward vs. leftward or upward vs. downward saccades, in terms of LFP mean amplitude in either hemisphere and regardless of the DBS status. Still, when comparing LFP mean amplitude between the baseline period and saccades in each direction, we found significant differences during DBS off only, namely, the right hemisphere LFP amplitude was significantly higher during right prosaccades (1.91 ± 0.41 vs. 1.48 ± 0.47; p=0.035), and the left hemisphere LFP amplitude was significantly higher during leftward prosaccades (2.06 ± 0.92 vs. 1.48 ± 0.47; p=0.047), when compared to baseline.

Notably, the right hemisphere LFP amplitude remained significantly lower than left hemisphere LFP amplitude for the entire saccade performance with DBS on (rightward (2.36±0.35 vs. 5.02±1.18), leftward (225±0.38 vs. 4.39±0.78; p=0.000), upward (2.13±0.31 vs. 4.03±0.95; p=0.000), and downward saccades (2.22±0.33 vs. 4.18±1.11; p=0.000), but not with DBS off, where such was attenuated.

Turning on the DBS had a clear effect on LFP amplitude, particularly in the left hemisphere. Right and left hemisphere LFP amplitude was significantly higher with DBS on than off (2.35±0.35 vs. 1.91±0.41; p=0.015 / 5.02±1.18 vs. 1.71±0.73; p=0.000) during rightward saccades. Left hemisphere LFP amplitude was significantly higher with DBS on than off (4.39±0.78 vs. 2.06±0.92; p=0.000) during leftward saccades, (4.34±0.76 vs. 1.48±0.47; p=0.000) horizontal baseline, (4.03±0.95 vs. 1.85±0.78; p=0.000) upward saccades, (4.18±1.11 vs. 2.04±0.87; p=0.001) downward saccades, (4.08±0.91 vs. 2.03±0.85; p=0.001) and vertical baseline.

Moreover, right hemisphere LFP amplitude positively correlated with latency of vertical saccades (R=0.61, p=0.009) with DBS on (Figure 4.15).
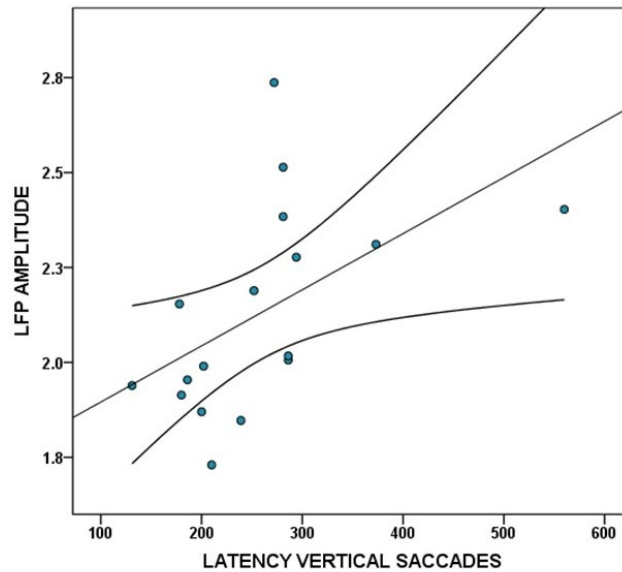
Figure 4.15: Correlation-plot between LFP amplitude of the right hemisphere with DBS on and saccade parameters.

Finally, left hemisphere LFP amplitude showed an interaction between DBS status (on vs. off) and saccade direction (rightward vs. leftward) (F=4.497; p=0.038), i.e., amplitude with DBS on became higher, more so for rightward saccades (Figure 4.16).
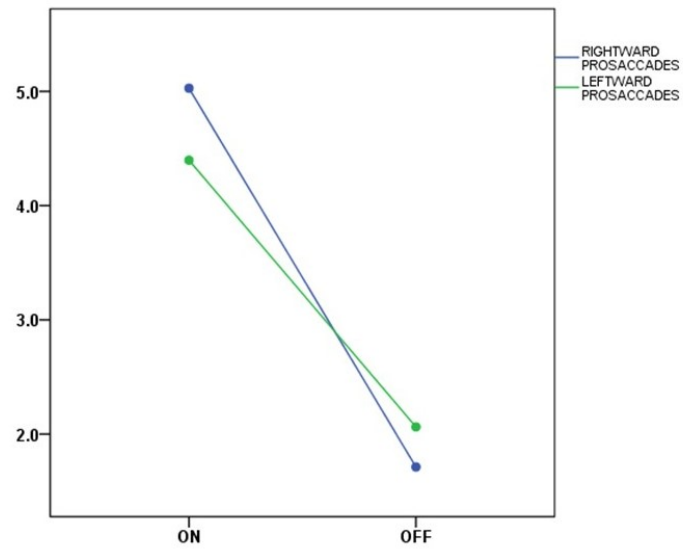
Figure 4.16: Interaction-plot between left hemisphere LFP amplitude (Y axis) and DBS status (X axis).

In sum, directional horizontal asymmetries were also seen in mean LFP amplitude, where greater amplitude was observed during execution of contralateral saccades when compared to baseline period.

5

Discussion and Conclusion

This exploratory study introduces an innovative approach to investigate eye movement-related activity in Parkinson's Disease (PD) by analyzing synchronized recordings from Deep Brain Stimulation (DBS) and Eye Tracking (ET), in real time.

The synchronization of the systems through Electroencephalography (EEG) was effectively achieved, demonstrating consistent reproducibility and accuracy across different data.

The clinical results enabled us to show that subthalamic nucleus (STN) neuronal populations seem to play a major role in the control of saccades. Horizontal saccades, at least, seem to show a directional bias in terms of brain activity, namely, one hemisphere seems to be predominantly concerned with the execution of contralateral saccades.

While this has been shown in animal neurophysiological studies and lesion studies in humans, evidence from contemporary research using functional magnetic resonance imaging (MRI) or magnetic transcortical electroencephalography have fallen short in putting in evidence the above claim [4]. One reason raised for such discrepancy deals with the fact that in the latter studies both excitatory and inhibitory activity might be influencing the imaging signal, thus precluding a clear assessment of each hemisphere's function [4]. Importantly, DBS seemed to have "restored" the aforementioned bias, by having decreased beta band potency in the left hemisphere during the execution of rightward saccades.

Interestingly, the patient's right hemibody has been predominantly affected during the course of the disease, suggesting a greater impairment of the left basal ganglia, which makes our results even more enlightening.

The local field potentials (LFP) amplitude analysis was roughly concordant with the above data, but particularly for conclusions drawn during DBS on periods, careful must be taken, as major technical artefacts by themselves, might have influenced the results, and data in this context might not only reflect saccade-related brain activity, but also electrode-induced artifacts.

The current research faces certain constraints. The primary limitation of the study is the small sample size, comprising only one participant with advanced-stage of PD affecting his ability to perform some eye movements correctly. This led to challenges during the tasks, possibly deviating from the average observed in a larger group of patients and impacting the accuracy of the findings. Also, it is obviously not possible to record from normal controls.

Moreover, the chosen eye movements paradigm resulted in a limited number of trials, impacting the statistical power of the analysis and the criteria for defining baseline and saccade periods differed from other eye movement paradigms, possibly influencing the different outcomes.

In conclusion, despite the presented difficulties, this novel approach, allowed for a simple, accurate and less invasive data recording providing crucial clinical information by comparing the directional activity of both brain hemispheres and investigating the differences between the activity with and without electrical stimulation. This opens new possibilities for investigating and optimizing the function of the eye movement network and the therapeutic potential of DBS in the context of eye movement disorders.

6

Future Work

While our study brings important novel data about the in vivo subcortical control of saccades in Parkinson's Disease (PD) patients and the influence of Deep Brain Stimulation (DBS), further research is needed to overcome the limitations and advance our understanding in this field.

Firstly, enhancing the robustness of our findings can be achieved by evaluating a larger number of patients and saccade trials, considering factors like age, sex, disease duration and further investigating electrode pairs of contacts initially chosen according to the influence of eye movements on beta band signal and not limb movement's influence.

In addition, the exploration of different frequency bands beyond the beta band, could provide a more complete understanding of the neural mechanisms underlying saccadic control in PD patients with DBS.

Due to time limitation in the execution of this work, our focus was narrowed down to investigating horizontal and vertical prosaccades with both DBS on and off. However, to draw more complete and extensive conclusions, it would be interesting to include an examination of the remaining types of eye movements in upcoming works.

Finally, it is suggested to analyze the EEG signal itself, together with the other systems, as the data is already time-synchronized. This integration can provide valuable cortical information on neuronal activity during the execution of eye movements. However, special attention should be given to eye muscle movement artifacts and to the selection of the most suitable EEG channel based on the brain's anatomical location of interest.

Bibliography

[1] World Health Organization. Parkinson Disease: A public health approach. *World Health Organization*, 291(3):390, 2022.

[2] Werner Poewe, Klaus Seppi, Caroline M. Tanner, Glenda M. Halliday, Patrik Brundin, Jens Volkmann, Anette-Eleonore Schrag, and Anthony E. Lang. Parkinson disease. *Nature reviews Disease primers*, 3(1):1–21, 2017.

[3] Jolande Fooken, Pooja Patel, Christina B. Jones, Martin J. McKeown, and Miriam Spering. Preservation of Eye Movements in Parkinson's Disease Is Stimulus- and Task-Specific. *The Journal of Neuroscience*, 42(3):487, jan 2022.

[4] J. Lemos, D. Pereira, L. Almendra, D. Rebelo, M. Patrício, J. Castelhano, G. Cunha, C. Januário, L. Cunha, A. Freire, and M. Castelo-Branco. Distinct functional properties of the vertical and horizontal saccadic network in Health and Parkinson's disease: An eye-tracking and fMRI study. *Brain Research*, 1648:469–484, oct 2016.

[5] Patrick Hickey and Mark Stacy. Deep brain stimulation: A paradigm shifting approach to treat parkinson's disease. *Frontiers in Neuroscience*, 10, 2016.

[6] James J. FitzGerald and Chrystalina A. Antoniades. Eye movements and deep brain stimulation. *Current opinion in neurology*, 29(1):69–73, 2016.

[7] Akihiro Yugeta, William D Hutchison, Clement Hamani, Utpal Saha, Andres M Lozano, Mojgan Hodaie, Elena Moro, Bogdan Neagu, and Robert Chen. Modulation of beta oscillations in the subthalamic nucleus with prosaccades and antisaccades in parkinson's disease. *The Journal of neuroscience : the official journal of the Society for Neuroscience*, 33(16):6895—6904, April 2013.

[8] Ling Tao, Quan Wang, Ding Liu, Jing Wang, Ziqing Zhu, and Li Feng. Eye tracking metrics to screen and assess cognitive impairment in patients with neurological disorders. *Neurological Sciences*, 41(7):1697–1704, July 2020.

[9] Michael Plöchl, José Ossandón, and Peter König. Combining eeg and eye tracking: identification, characterization, and correction of eye movement artifacts in electroencephalographic data. *Frontiers in Human Neuroscience*, 6, 2012.

[10] Elena Pretegiani and Lance M. Optican. Eye Movements in Parkinson's Disease and Inherited Parkinsonian Syndromes. *Frontiers in Neurology*, 8:592, 2017.

[11] Antonina Kouli, Kelli M. Torsney, and Wei-Li Kuan. *Parkinson's Disease: Etiology, Neuropathology, and Pathogenesis. In T. B. Stoker (Eds.) et. al., Parkinson's Disease: Pathogenesis and Clinical Aspects. Chapter 1.* Codon Publications, Brisbane (AU), 2018.

[12] Sílvia Cristina and Castro Alves. Fisiopatologia dos Gânglios da Base na Doença de Parkinson. Master's thesis, Faculdade de Medicina da Universidade de Coimbra, Coimbra, mar 2012.

[13] George DeMaagd and Ashok Philip. Parkinson's disease and its management: Part 1: Disease entity, risk factors, pathophysiology, clinical presentation, and diagnosis. *PT*, 40(8), 2015.

[14] Fabio Blandini, Giuseppe Nappi, Cristina Tassorelli, and Emilia Martignoni. Functional changes of the basal ganglia circuitry in parkinson's disease. *Progress in Neurobiology*, 62(1):63–88, 2000.

[15] Jonathan W. Mink. Chapter 30 - the basal ganglia. In Larry R. Squire, Darwin Berg, Floyd E. Bloom, Sascha du Lac, Anirvan Ghosh, and Nicholas C. Spitzer, editors, *Fundamental Neuroscience (Fourth Edition)*, pages 653–676. Academic Press, San Diego, fourth edition edition, 2013.

[16] Dag Aarsland, Lucia Batzu, Glenda M. Halliday, Gert J. Geurtsen, Clive Ballard, K. Ray Chaudhuri, and Daniel Weintraub. Parkinson disease-associated cognitive impairment. *Nature reviews Disease primers*, 2021.

[17] Launch of WHO's Parkinson disease technical brief. https://www.who.int/news/item/14-06-2022-launch-of-who-s-parkinson-disease-technical-brief. 2023-01-18.

[18] Philippe Rizek, Niraj Kumar, and Mandar S. Jog. An update on the diagnosis and treatment of parkinson disease. *Canadian medical association journal*, 188(16), 2016.

[19] Pablo Martinez-Martin, Carmen Rodriguez-Blazquez, Mario Alvarez-Sanchez, Tomoko Arakaki, Alberto Bergareche-Yarza, Anabel Chade, Nelida Garretto, Oscar Gershanik, Monica M. Kurtis, Juan Carlos Martinez-Castrillo, Amelia Mendoza-Rodriguez, Henry P. Moore, Mayela Rodriguez-Violante, Carlos Singer, Barbara C. Tilley, Jing Huang, Glenn T. Stebbins, and Christopher G. Goetz. Expanded and independent validation of the Movement Disorder Society-Unified Parkinson's Disease Rating Scale (MDS-UPDRS). *Journal of Neurology*, 260(1):228–236, jan 2013.

[20] Eduardo Tolosa, Alicia Garrido, Sonja W Scholz, and Werner Poewe. Challenges in the diagnosis of parkinson's disease. *Lancet neurology journal*, 20(5), 2021.

[21] Roberta Balestrino and AHV Schapira. Parkinson disease. *European journal of neurology*, 27(1):27–42, 2020.

[22] Maja Klarendic and Diego Kaski. Deep brain stimulation and eye movements. *European Journal of Neuroscience*, 53(7), 2021.

[23] Maria Eliza Freitas, Christopher W. Hess, and Susan H. Fox. *Seminars in neurology*, 37(2), 2017.

[24] Benabid A.L., Pollak P., Louveau A., Henry S., and de Rougemont J. Combined (thalamotomy and stimulation) stereotactic surgery of the VIM thalamic nucleus for bilateral Parkinson disease. *Applied neurophysiology*, 50(1-6):344–346, 1987.

[25] John Gardner. A history of deep brain stimulation: Technological innovation and the role of clinical assessment tools. *Social Studies of Science*, 43(5), 2013.

[26] Deep Brain Stimulation — Parkinson's Disease. https://www.michaeljfox.org/deep-brain-stimulation. 2022-10-29.

[27] Image provided by Medtronic, Inc. Private Communication. 2023-2-01.

[28] Tiago Matheus Nordi, Rodrigo Henrique Gounella, Maximiliam Luppe, João Navarro Soares Junior, Erich Talamoni Fonoff, Eduardo Colombari, Murilo Araujo Romero, and João Paulo Pereira do Carmo. Low-noise amplifier for deep-brain stimulation (dbs). *Electronics*, 11(6), 2022.

[29] Deep Brain Stimulation (DBS) - Parkinson's Community. https://parkinsons.community/deep-brain-stimulation-dbs/. 2022-11-05.

[30] Robert F. Dallapiazza, Philippe De Vloo, Anton Fomenko, Darrin J. Lee, Clement Hamani, Renato P. Munhoz, Mojgan Hodaie, Andres M. Lozano, Alfonso Fasano, and Suneil K. Kalia. Considerations for Patient and Target Selection in Deep Brain Stimulation Surgery for Parkinson's Disease. *Parkinson's Disease: Pathogenesis and Clinical Aspects*, pages 145–160, dec 2018.

[31] Helen Bronte-stewart. *Deep Brain Stimulation Management: Surgical placement of deep brain stimulating leads for the treatment of movement disorders – intraoperative aspects: physiological mapping, test stimulation, and patient evaluation.* Cambridge University Press, University of California, San Francisco, second edition, 2015.

[32] Zixiao Yin, Guanyu Zhu, Baotian Zhao, Yutong Bai, Yin Jiang, Wolf-Julian Neumann, Andrea A. Kühn, and Jianguo Zhang. Local field potentials in parkinson's disease: A frequency-based review. *Neurobiology of Disease*, 155:105372, 2021.

[33] Medtronic (Private communication). Scientific compendium: Research on brain sensing and brainsense™ technology.

[34] Florencia Sanmartino, Álvaro J. Cruz-Gómez, Raúl Rashid-López, Elena Lozano-Soto, Fernando López-Sosa, Amaya Zuazo, Jesús Riqué-Dormido, Raúl Espinosa-Rosso, and Javier J. González-Rosa. Subthalamic beta activity in parkinson's disease may be linked to dorsal striatum gray matter volume and prefrontal cortical thickness: A pilot study. *Frontiers in Neurology*, 13, 2022.

[35] John Y. Fang and Christopher Tolleson. The role of deep brain stimulation in Parkinson's disease: an overview and update on new developments. *Neuropsychiatric Disease and Treatment*, 13:723, mar 2017.

[36] Patrick Hickey and Mark Stacy. Deep brain stimulation: A paradigm shifting approach to treat parkinson's disease. *Frontiers in Neuroscience*, 10, 04 2016.

[37] John E. Fleming, Eleanor Dunn, and Madeleine M. Lowery. Simulation of closed-loop deep brain stimulation control schemes for suppression of pathological beta oscillations in parkinson's disease. *Frontiers in Neuroscience*, 14, 2020.

[38] Walid Bouthour, Pierre Megevand, John Donoghue, Christian Luscher, Niels Birbaumer, and Paul Krack. Biomarkers for closed-loop deep brain stimulation in Parkinson disease and beyond. *Nature Reviews Neurology 2019 15:6*, 15(6):343–352, apr 2019.

[39] Joohi Jimenez-Shahed. Device profile of the percept pc deep brain stimulation system for the treatment of parkinson's disease and related disorders. *Expert Review of Medical Devices*, 18(4):319–332, 2021. PMID: 33765395.

[40] Medtronic (Private communication). BrainSense ™ Technology : Published Use-Case Examples and Expert Standard deviation.

[41] Medtronic (Private communication). Brainsense™ Technology summary.

[42] Deep Brain Stimulation Systems Percept PC Medtronic. https://europe.medtronic.com/xd-en/healthcare-professionals/products/neurological/deep-brain-stimulation-systems/percept-pc.html. 2022-11-05.

[43] Joohi Jimenez-Shahed. Device profile of the percept PC deep brain stimulation system for the treatment of Parkinson's disease and related disorders. *Review of Medical Devices*, 2021.

[44] R. John Leigh and David S. Zee. *The Neurology of Eye Movements*. Oxford University Press, 6 2015.

[45] Martin Gorges, Hans-peter Muller, and Jan Kassubek. Structural and Functional Brain Mapping Correlates of Impaired Eye Movement Control in Parkinsonian Syndromes : A Systems-Based Concept. *Frontiers in Neurology*, 9, 2018.

[46] Dale Purves, George J Augustine, David Fitzpatrick, Lawrence C Katz, Anthony-Samuel LaMantia, James O McNamara, and S Mark Williams. Types of Eye Movements and Their Functions. 2001.

[47] Microsaccades are triggered by low retinal image slip. *Proceedings of the National Academy of Sciences of the United States of America*, 103(18):7192–7197, may 2006.

[48] Lucyna Schalén. Quantification of tracking eye movements in normal subjects. *Acta otolaryngologica*, 90(5-6):404–413, 1980.

[49] Benjamin T. Carter and Steven G. Luke. Best practices in eye tracking research. *International Journal of Psychophysiology*, 155:49–62, sep 2020.

[50] Anshul Srivastava, Ratna Sharma, Sanjay K Sood, Garima Shukla, Vinay Goyal, and Madhuri Behari. Saccadic eye movements in parkinson's disease. *Indian Journal of ophthalmology*, 62(5), 2014.

[51] Elena Pretegiani and Lance M. Optican. Eye movements in parkinson's disease and inherited parkinsonian syndromes. *Frontiers in Neurology*, 8, 2017.

[52] Jolande Fooken, Pooja Patel, Christina B. Jones, Martin J. McKeown, and Miriam Spering. Preservation of Eye Movements in Parkinson's Disease Is Stimulus- and Task-Specific. *Journal of Neuroscience*, 42(3):487–499, jan 2022.

[53] Ling Tao, Quan Wang, Ding Liu, Jing Wang, Ziqing Zhu, and Li Feng. Eye tracking metrics to screen and assess cognitive impairment in patients with neurological disorders. *Neurological Sciences*, 41(7):1697–1704, jul 2020.

[54] Eye Tracking 101: What Is It How Does It Work In Real Life? - Eyeware. https://eyeware.tech/blog/what-is-eye-tracking/. 2022-11-06.

[55] EyeLink 1000 Plus - The Most Flexible Eye Tracker - SR Research. https://www.sr-research.com/eyelink-1000-plus/. 2022-11-17.

[56] About eye tracking - fast, accurate, reliable eye tracking. https://www.sr-research.com/about-eye-tracking. 01-10-2022.

[57] EyeLink portable duo The EyeLink 1000 Plus Eye Tracker. https://www.sr-research.com/wp-content/uploads/2018/01/EyeLink-1000-Plus-Brochure.pdf. 2022-11-17.

[58] Electroencephalogram (EEG) - NHS. https://www.nhs.uk/conditions/electroencephalogram/. 31-10-2022.

[59] Mona Sazgar and Michael G. Young. Overview of EEG, Electrode Placement, and Montages. *Absolute Epilepsy and EEG Rotation Review*, pages 117–125, 2019.

[60] ROUTINE EEG - NeuroEvolution - EEG, SEEG, EMG, PSG, TCD IONM. https://neuroevolution.pt/brainquick-clinical-eeg-routine-eeg/. 01-02-2023.

[61] Qing Wang, Lin Meng, Jun Pang, Xiaodong Zhu, and Dong Ming. Characterization of EEG Data Revealing Relationships With Cognitive and Motor Symptoms in Parkinson's Disease: A Systematic Review. *Frontiers in Aging Neuroscience*, 12:373, nov 2020.

[62] J. A. Nij Bijvank, A. Petzold, L. J. Balk, H. S. Tan, B. M. J. Uitdehaag, M. Theodorou, and L. J. van Rijn. A standardized protocol for quantification of saccadic eye movements: DEMoNS. *PLoS ONE*, 13(7):1–19, 2018.

[63] Francisco Cidade. From Basic Research to the Clinic: Creation of an Interface for Analysis of Eye Movements. Master's thesis, Faculdade de Ciências e Tecnologia da Universidade de Coimbra, Coimbra, To be submited.

[64] Michael Plöchl, José Ossandón, and Peter König. A removal of eye movement and blink artifacts from eeg data using morphological component analysis. *Computational and Mathematical Methods in Medicine*, 2017.

[65] Melanie Mruk, Ralf Stroop, Jan Boergel, Norbert M. Lang, Makoto Nakamura, Ralph Lehrke, and Samer Zawy Alsofy. Neurostimulator-induced ecg artefacts: A systematic analysis. *Clinical Neurology and Neurosurgery*, 203:106557, 2021.

[66] M.J. Stam, B.C.M. Van Wijk, P. Sharma, M. Beudel, D.A. Piña-Fuentes, R.M.A. De Bie, P.R. Schuurman, W.J. Neumann, and A.W.G. Buijink. A comparison of methods to suppress electrocardiographic artifacts in local field potential recordings. *Clinical Neurophysiology*, 146:147–161, 2023.

[67] Joshua K Wong, Jackson N Cagle, Stephanie Cernera, Wayne K Goodman WayneGoodman, Michaela E Alarie, Nicole R Provenza, Michelle Avendano-Ortega, Sarah A McKay, Ayan S Waite, Raissa K Mathura, Jeffrey A Herron, Sameer A Sheth, David A Borton, and Wayne K Goodman. Artifact characterization and mitigation techniques during concurrent sensing and stimulation using bidirectional deep brain stimulation platforms. *Front. Hum. Neurosci*, 16:1016379, 2022.

[68] Sanjeev Jain and Dr Rai. Blind source separation and ICA techniques: a review. *IJEST*, 4, 2012.

[69] Victoria Peterson, Timon Merk, Alan Bush, Vadim Nikulin, Andrea A. Kuhn, Wolf Julian Neumann, and R. Mark Richardson. Movement decoding using spatio-spectral features of cortical and subcortical local field potentials. *Experimental Neurology*, 359:114261, jan 2023.

[70] Mateo Tobón-Henao, Andrés Álvarez Meza, and Germán Castellanos-Dominguez. Subject-Dependent Artifact Removal for Enhancing Motor Imagery Classifier Performance under Poor Skills. *Sensors*, 22(15), 2022.

[71] Andrea A. Kühn, David Williams, Andreas Kupsch, Patricia Limousin, Marwan Hariz, Gerd Helge Schneider, Kielan Yarrow, and Peter Brown. Event-related beta desynchronization in human subthalamic nucleus correlates with motor performance. *Brain*, 127(4):735–746, 2004.

[72] Aasef G. Shaikh, Chrystalina Antoniades, James Fitzgerald, and Fatema F. Ghasia. Effects of deep brain stimulation on eye movements and vestibular function. *Frontiers in Neurology*, 9, 2018.

[73] James J. FitzGerald and Chrystalina A. Antoniades. Eye movements and deep brain stimulation. *Current opinion in neurology*, 29(1):69–73, 2016.

[74] Vladimir Litvak, Esther Florin, Gertrúd Tamás, Sergiu Groppa, and Muthuraman Muthuraman. EEG and MEG primers for tracking DBS network effects. *NeuroImage*, 224:117447, jan 2021.

[75] Boleslaw Jaskula, Krzysztof Pancerz, and Jaroslaw Szkola. Toward Synchronization of EEG and Eye-tracking Data Using an Expert System Extended Abstract. *University of Information Technology and Management Sucharskiego Str. 2, 35-225 Rzeszow, Poland*, pages 196–198, 2015.

[76] Olaf Dimigen, Werner Sommer, Annette Hohlfeld, Arthur M. Jacobs, and Reinhold Kliegl. Coregistration of eye movements and EEG in natural reading: Analyses and review. *Journal of Experimental Psychology: General*, 140(4):552–572, nov 2011.

[77] Eye Tracking and EEG - Fast, Accurate, Reliable Eye Tracking. https://www.sr-research.com/eye-tracking-blog/background/eye-tracking-and-eeg/. 2023-01-25.

[78] TTL Signalling Synchronization. https://www.sr-research.com/support/thread-81.html. 2023-01-25.

[79] Arnaud Delorme and Scott Makeig. Eeglab: an open-source toolbox for analysis of single-trial eeg dynamics including independent component analysis. *Journal of Neuroscience Methods*, 134(1):9–21, Mar 2004.

[80] Elena Pretegiani and Lance M. Optican. Eye movements in Parkinson's disease and inherited parkinsonian syndromes. *Frontiers in Neurology*, 8:592, 2017.

[81] Atefeh Asadi, Mojtaba Madadi Asl, Abdol-Hossein Vahabie, and Alireza Valizadeh. The Origin of Abnormal Beta Oscillations in the Parkinsonian Corticobasal Ganglia Circuits. *Hindawi, Parkinson's Disease*, 2022.

[82] Jacopo Barone and Holly E. Rossiter. Understanding the Role of Sensorimotor Beta Oscillations. *Frontiers in Systems Neuroscience*, 15:655886, may 2021.

[83] Bernhard Spitzer and Saskia Haegens. Cognition and Behavior Beyond the Status Quo: A Role for Beta Oscillations in Endogenous Content (Re)Activation. *eNeuro Cognition and Behavior*, 2017.

[84] Giulia Giannini, Luca Baldelli, Gaetano Leogrande, Ilaria Cani, Paolo Mantovani, Giovanna Lopane, Pietro Cortelli, Giovanna Calandra-Buonaura, and Alfredo Conti. Case report: Bilateral double beta peak activity is influenced by stimulation, levodopa concentrations, and motor tasks, in a Parkinson's disease patient on chronic deep brain stimulation. *Frontiers in Neurology*, 14:1163811, may 2023.

[85] Atefeh Asadi, Mojtaba Madadi Asl, Abdol-Hossein Vahabie, and Alireza Valizadeh. The Origin of Abnormal Beta Oscillations in the Parkinsonian Corticobasal Ganglia Circuits. *The Journal of neuroscience : the official journal of the Society for Neuroscience*, 2022.

[86] Experiment Builder for Eye-Tracking Experiments - SR Research. https://www.sr-research.com/experiment-builder/. 2023-05-15.

[87] Image provided by Medtronic, Inc. Personal Communication. 2022-7-01.

Appendices

A

Supplementary Results

Table A.1: Horizontal prosaccades eye movement metrics results with Deep Brain Stimulation (DBS) on and off. Notably, certain eye movement metric trials have recorded values of zero, indicating potential instances of missed saccades or signal disruptions, likely due to factors like blinking or temporary signal loss.

Horizontal Prosaccades Left Eye Gaze	DBS ON			DBS OFF		
	Latency (ms)	Peak Velocity (deg/s)	Gain	Latency (ms)	Peak Velocity (deg/s)	Gain
Right target 1	382	501,761	1,038	0	0,000	0,000
Right target 2	0	0,000	0,000	207	451,726	0,941
Right target 3	249	528,881	0,968	194	528,718	0,853
Right target 4	209	511,784	0,968	260	377,237	1,109
Right target 5	0	0,000	0,000	0	0,000	0,000
Right target 6	182	480,832	0,967	0	0,000	0,000
Right target 7	0	0,000	0,000	185	256,696	0,457
Right target 8	265	524,009	1,003	135	403,648	0,872
Right target 9	189	492,336	0,852	299	457,944	0,936
Right target 10	127	454,390	0,756	0	0,000	0,000
Right target 11	0	0,000	0,000	221	328,072	0,581
Right target 12	171	533,258	1,068	425	582,990	1,035
Right target 13	263	383,843	0,642	234	355,264	0,927
Right target 14	189	513,154	0,936	0	0,000	0,000
Right target 15	137	321,327	0,841	0	0,000	0,000
Right target 16	252	438,462	0,849	292	458,032	0,903
Average Right Target	218	473,670	0,907	245	420,033	0,861
PSD Right Target	66,7	62,063	0,118	76,3	91,479	0,187
Left target 1	211	467,999	1,033	256	473,728	0,808
Left target 2	208	427,544	0,970	299	468,861	0,982
Left target 3	207	461,295	0,983	176	465,718	0,860
Left target 4	314	537,151	1,004	643	395,681	1,019
Left target 5	302	424,409	1,063	521	268,696	0,635
Left target 6	319	408,512	0,924	0	0,000	0,000
Left target 7	377	446,948	0,977	203	444,170	0,986
Left target 8	176	442,647	0,930	0	0,000	0,000
Left target 9	201	489,851	0,950	224	366,514	0,594
Left target 10	0	0,000	0,000	0	0,000	0,000
Left target 11	0	0,000	0,000	741	436,960	0,939
Left target 12	403	503,180	0,990	0	0,000	0,000
Left target 13	255	465,086	1,144	184	382,102	0,831
Left target 14	349	423,130	0,983	0	0,000	0,000
Left target 15	0	0,000	0,000	487	450,566	0,966
Left target 16	306	481,889	0,992	761	375,329	0,000
Average Left Target	279	459,972	0,996	409	411,666	0,862
PSD Left Target	71,3	35,170	0,056	218,4	58,917	0,141

Table A.2: Vertical prosaccades eye movement metrics results with DBS on and off. Notably, certain eye movement metric trials have recorded values of zero, indicating potential instances of missed saccades or signal disruptions, likely due to factors like blinking or temporary signal loss.

Vertical Prosaccades Left Eye Gaze	DBS ON			DBS OFF		
	Latency (ms)	Peak Velocity (deg/s)	Gain	Latency (ms)	Peak Velocity (deg/s)	Gain
Up target 1	0	0,000	0,000	285	383,590	0,741
Up target 2	0	0,000	0,000	578	340,272	0,962
Up target 3	0	0,000	0,000	254	403,518	0,947
Up target 4	373	371,209	0,888	271	284,232	0,770
Up target 5	0	0,000	0,000	0	0,000	0,000
Up target 6	286	306,020	1,009	0	0,000	0,000
Up target 7	180	271,223	1,045	0	0,000	0,000
Up target 8	0	0,000	0,000	0	0,000	0,000
Up target 9	0	0,000	0,000	492	431,360	0,971
Up target 10	0	0,000	0,000	0	0,000	0,000
Up target 11	178	421,611	1,030	0	0,000	0,000
Up target 12	0	0,000	0,000	0	0,000	0,000
Up target 13	252	385,389	0,806	0	0,000	0,000
Up target 14	186	0,000	0,000	0	0,000	0,000
Up target 15	0	258,978	0,772	0	0,000	0,000
Up target 16	200	271,765	0,712	554	373,232	0,742
Average Up Target	236	326,599	0,894	406	369,367	0,855
PSD Up Target	67,4	60,407	0,126	138,4	47,119	0,105
Down target 1	0	0,000	0,000	0	0,000	0,000
Down target 2	0	0,000	0,000	408	393,711	0,804
Down target 3	0	0,000	0,000	300	292,408	0,542
Down target 4	0	0,000	0,000	0	0,000	0,000
Down target 5	281	298,977	0,643	356	288,296	0,520
Down target 6	560	271,199	0,581	0	0,000	0,000
Down target 7	202	349,514	0,596	404	382,297	0,727
Down target 8	210	230,396	0,543	0	0,000	0,000
Down target 9	272	188,687	0,540	450	384,283	0,766
Down target 10	0	0,000	0,000	0	0,000	0,000
Down target 11	281	317,028	0,608	724	238,273	0,620
Down target 12	294	210,403	0,482	359	300,190	0,591
Down target 13	239	268,881	0,617	540	402,249	0,791
Down target 14	0	0,000	0,000	650	350,475	0,880
Down target 15	131	415,850	0,662	0	0,000	0,000
Down target 16	286	232,386	0,535	783	274,675	0,000
Average Down Target	276	278,332	0,581	412	330,686	0,694
PSD Down Target	106,5	65,652	0,053	206,6	55,580	0,121

Table A.3: Calculation of the beta band power graph integral between 25-30Hz and 20-30Hz for horizontal prosaccades with DBS on and off in both hemispheres.

Horizontal Prosaccades Left Eye Gaze	DBS ON				DBS OFF			
	Integral of the beta band power graph (25-30 Hz)		Integral of the beta band power graph (20-30 Hz)		Integral of the beta band power graph (25-30 Hz)		Integral of the beta band power graph (20-30 Hz)	
	Right Hemisphere	Left Hemisphere	Right Hemisphere	Left Hemisphere	Right Hemisphere	Left Hemisphere	Right Hemisphere	Left Hemisphere
Right target 1	0,721	0,917	0,9468	0,7403	0,7715	0,7663	0,9473	0,8603
Right target 2	0,584	0,598	0,993	0,951	0,788	0,661	0,910	0,943
Right target 3	0,710	0,713	0,910	0,888	0,706	0,805	0,742	0,969
Right target 4	0,969	0,806	0,841	0,978	0,671	0,888	0,942	0,969
Right target 5	0,788	0,673	0,786	0,636	0,853	0,864	0,914	0,700
Right target 6	0,601	0,740	0,969	0,720	0,981	0,906	0,995	1,005
Right target 7	0,845	0,570	0,776	0,881	0,702	0,900	0,903	0,814
Right target 8	0,726	0,873	0,945	0,737	0,684	0,798	0,885	0,752
Right target 9	0,882	0,669	0,833	0,926	0,588	0,712	0,858	0,897
Right target 10	0,717	0,649	0,930	0,871	0,963	0,749	0,663	1,004
Right target 11	0,710	0,946	0,961	0,958	0,959	0,806	0,729	0,751
Right target 12	0,925	0,853	0,729	0,840	0,775	0,826	0,991	1,008
Right target 13	0,615	0,744	0,861	0,673	0,697	0,762	0,935	0,953
Right target 14	0,701	0,606	0,858	0,873	0,646	0,905	0,868	0,884
Right target 15	0,903	0,703	0,944	0,894	0,866	0,844	0,892	1,000
Right target 16	0,937	0,596	0,898	0,820	0,688	0,826	0,939	0,722
Average Right Target	0,771	0,728	0,886	0,837	0,771	0,814	0,882	0,889
PSD Right Target	0,121	0,116	0,075	0,102	0,117	0,069	0,091	0,106
Left target 1	0,646	0,923	0,869	0,937	0,929	0,849	0,880	0,895
Left target 2	0,5568	0,838	0,765	0,761	0,5793	0,658	0,957	0,920
Left target 3	0,770	0,790	0,956	0,901	0,631	0,616	0,939	0,931
Left target 4	0,954	0,619	0,948	0,886	0,629	0,694	0,838	0,926
Left target 5	0,843	0,925	0,916	0,958	0,646	0,904	0,957	0,889
Left target 6	0,724	0,598	0,726	0,979	0,574	0,865	0,961	0,991
Left target 7	0,970	0,632	0,899	0,738	0,567	0,926	0,948	0,972
Left target 8	0,629	0,797	0,848	0,927	0,745	0,680	0,941	0,922
Left target 9	0,682	0,645	0,983	0,729	0,760	0,803	0,991	0,926
Left target 10	0,655	0,814	0,960	0,947	0,973	0,720	0,691	0,785
Left target 11	0,709	0,723	0,990	0,934	0,636	0,907	0,987	0,850
Left target 12	0,784	0,950	0,881	0,995	0,589	0,897	0,897	0,945
Left target 13	0,886	0,730	0,849	0,994	0,602	0,718	0,889	0,947
Left target 14	0,558	0,856	0,943	0,971	0,683	0,765	0,803	0,913
Left target 15	0,686	0,657	0,860	0,913	0,914	0,917	0,953	0,756
Left target 16	0,703	0,787	0,989	1,003	0,816	0,737	0,918	0,818
Average Left Target	0,735	0,768	0,899	0,911	0,705	0,791	0,909	0,899
PSD Left Target	0,122	0,111	0,075	0,087	0,132	0,101	0,075	0,063

Table A.4: Calculation of the beta band power graph integral between 25-30Hz and 20-30Hz for the baseline periods between horizontal saccades, with DBS on and off, in both hemispheres.

Horizontal Prosaccades Left Eye Gaze	DBS ON				DBS OFF			
	Integral of the beta band power graph (25-30 Hz)		Integral of the beta band power graph (20-30 Hz)		Integral of the beta band power graph (25-30 Hz)		Integral of the beta band power graph (20-30 Hz)	
	Right Hemisphere	Left Hemisphere	Right Hemisphere	Left Hemisphere	Right Hemisphere	Left Hemisphere	Right Hemisphere	Left Hemisphere
Center target 1	0,741	0,865	0,875	0,998	0,605	0,650	0,869	0,918
Center target 2	0,965	0,823	0,773	0,840	0,629	0,860	0,808	0,841
Center target 3	0,997	0,719	0,846	0,851	0,873	0,973	0,709	0,877
Center target 4	0,735	0,803	0,886	0,943	0,754	0,735	0,889	0,995
Center target 5	0,642	0,864	0,893	0,905	0,691	0,753	0,872	0,945
Center target 6	0,839	0,671	0,826	1,003	0,973	0,864	0,821	0,899
Center target 7	0,547	0,645	0,887	0,751	0,528	0,785	0,833	0,879
Center target 8	0,836	0,657	0,979	0,894	0,870	0,548	0,979	0,875
Center target 9	0,599	0,872	0,936	0,733	0,872	0,696	0,950	0,942
Center target 10	0,898	0,855	0,882	0,754	0,960	0,821	0,795	0,933
Center target 11	0,795	0,851	0,781	0,863	0,708	0,564	0,982	0,757
Center target 12	0,631	0,682	0,950	0,969	0,711	0,766	0,902	0,805
Center target 13	0,991	0,746	0,854	0,749	0,538	0,832	0,957	0,825
Center target 14	0,605	0,803	0,941	0,866	0,552	0,632	1,010	0,958
Center target 15	0,767	0,734	0,906	0,905	0,697	0,780	1,011	0,839
Center target 16	0,585	0,691	0,709	0,705	0,748	0,812	0,962	0,964
Center target 17	0,630	0,579	0,972	1,010	0,861	0,826	1,007	0,956
Center target 18	0,809	0,786	0,847	0,833	0,600	0,697	0,985	0,988
Center target 19	0,903	0,979	0,756	0,993	0,614	0,874	0,855	0,818
Center target 20	0,881	0,749	0,953	0,893	0,865	0,808	0,878	0,908
Center target 21	0,659	0,851	0,930	0,847	0,629	0,994	0,998	0,789
Center target 22	0,780	0,885	0,742	0,877	0,897	0,696	0,908	0,732
Center target 23	0,739	0,875	0,990	0,814	0,748	0,568	0,916	0,947
Center target 24	0,705	0,830	0,893	0,826	0,953	0,853	0,933	0,984
Center target 25	0,858	0,957	0,937	0,900	0,851	0,822	0,997	0,985
Center target 26	0,750	0,574	0,843	0,966	0,856	0,712	0,809	0,891
Center target 27	0,718	0,729	0,626	0,872	0,733	0,670	0,987	0,794
Center target 28	0,831	0,850	0,828	0,814	0,542	0,853	0,892	1,004
Center target 29	0,801	0,951	1,007	0,899	0,677	0,834	0,918	0,908
Center target 30	0,749	0,694	0,846	0,959	0,716	0,710	0,972	0,747
Center target 31	0,540	0,873	0,767	0,878	0,656	0,722	0,916	0,926
Center target 32	0,845	0,836	0,911	0,986	0,759	0,939	0,648	0,963
Average Center Target	0,762	0,790	0,868	0,878	0,739	0,770	0,905	0,893
PSD CenterTarget	0,123	0,103	0,087	0,082	0,130	0,110	0,087	0,077

Table A.5: Calculation of the beta band power graph integral between 25-30Hz and 20-30Hz for vertical prosaccades with DBS on and off in both hemispheres.

Vertical Prosaccades Left Eye Gaze	DBS ON				DBS OFF			
	Integral of the beta band power graph (25-30 Hz)		Integral of the beta band power graph (20-30 Hz)		Integral of the beta band power graph (25-30 Hz)		Integral of the beta band power graph (20-30 Hz)	
	Right Hemisphere	Left Hemisphere	Right Hemisphere	Left Hemisphere	Right Hemisphere	Left Hemisphere	Right Hemisphere	Left Hemisphere
Up target 1	0,949	0,756	0,9248	0,9596	0,7218	0,9235	0,9025	0,65
Up target 2	0,899	0,763	0,811	0,989	0,629	0,620	0,712	0,950
Up target 3	0,831	0,548	0,575	0,926	0,695	0,814	0,978	0,897
Up target 4	0,619	0,668	0,847	0,969	0,639	0,712	0,862	0,828
Up target 5	0,615	0,653	0,871	0,938	0,717	0,816	0,954	0,910
Up target 6	0,577	0,881	0,731	0,780	0,939	0,978	0,970	0,869
Up target 7	0,753	0,549	0,926	0,802	0,875	0,587	0,821	0,913
Up target 8	0,833	0,716	0,957	0,996	0,752	0,776	0,824	0,904
Up target 9	0,818	0,693	0,937	0,693	0,835	0,850	0,965	0,913
Up target 10	0,799	0,756	0,987	0,975	0,868	0,786	0,760	0,791
Up target 11	0,849	0,779	0,993	0,886	0,742	0,721	0,862	0,995
Up target 12	0,834	0,605	0,970	0,975	0,751	0,859	0,864	0,983
Up target 13	0,904	0,584	0,832	0,987	0,724	0,670	0,980	0,889
Up target 14	0,779	0,801	0,718	0,936	0,713	0,736	0,965	0,996
Up target 15	0,657	0,709	0,953	0,833	0,645	0,793	0,975	0,759
Up target 16	0,768	0,904	0,817	0,865	0,690	0,653	0,726	0,929
Average Up Target	0,780	0,710	0,866	0,907	0,746	0,768	0,883	0,886
PSD Up Target	0,107	0,103	0,112	0,086	0,087	0,104	0,090	0,089
Down target 1	0,643	0,929	0,988	0,888	0,746	0,900	0,893	0,990
Down target 2	0,707	0,687	0,792	0,748	0,8104	0,897	0,770	0,999
Down target 3	0,657	0,945	0,866	0,840	0,767	0,742	0,900	0,923
Down target 4	0,907	0,565	0,696	0,917	0,735	0,822	0,968	0,883
Down target 5	0,787	0,804	0,887	0,969	0,652	0,604	0,906	0,937
Down target 6	0,706	0,540	0,692	0,824	0,833	0,684	0,941	0,949
Down target 7	0,618	0,823	0,722	0,866	0,939	0,576	0,743	0,742
Down target 8	0,679	0,568	0,819	0,853	0,799	0,954	1,009	0,863
Down target 9	0,613	0,720	0,923	0,853	0,631	0,720	0,568	0,942
Down target 10	0,590	0,616	0,848	0,884	0,929	0,549	0,853	1,010
Down target 11	0,835	0,628	0,684	0,892	0,629	0,725	0,989	0,768
Down target 12	0,747	0,562	0,879	0,891	0,694	0,761	0,848	0,879
Down target 13	0,850	0,666	0,983	0,731	0,911	0,792	0,801	0,883
Down target 14	0,601	0,840	0,959	0,657	0,568	0,831	0,712	0,803
Down target 15	0,961	0,750	0,803	0,868	0,569	1,000	0,842	0,814
Down target 16	0,850	0,876	0,769	0,635	0,936	0,704	0,977	0,944
Average Down Target	0,735	0,720	0,832	0,832	0,759	0,766	0,857	0,896
PSD Down Target	0,114	0,132	0,099	0,090	0,124	0,127	0,114	0,079

Table A.6: Calculation of the beta band power graph integral between 25-30Hz and 20-30Hz for the baseline periods between vertical saccades, with DBS on and off, in both hemispheres.

Vertical Prosaccades Left Eye Gaze	DBS ON				DBS OFF			
	Integral of the beta band power graph (25-30 Hz)		Integral of the beta band power graph (20-30 Hz)		Integral of the beta band power graph (25-30 Hz)		Integral of the beta band power graph (20-30 Hz)	
	Right Hemisphere	Left Hemisphere	Right Hemisphere	Left Hemisphere	Right Hemisphere	Left Hemisphere	Right Hemisphere	Left Hemisphere
Center target 1	0,767	0,858	0,982	0,825	0,894	0,926	0,800	0,952
Center target 2	0,788	0,920	0,980	0,943	0,701	0,960	0,760	0,943
Center target 3	0,751	0,677	0,882	0,924	0,649	0,833	1,000	0,685
Center target 4	0,865	0,886	0,904	0,818	0,856	0,894	0,859	0,801
Center target 5	0,646	0,605	0,621	0,961	0,872	0,809	0,739	0,898
Center target 6	0,635	0,893	0,922	0,908	0,779	0,885	0,977	0,951
Center target 7	0,682	0,935	0,770	0,778	0,851	0,862	0,926	0,950
Center target 8	0,747	0,874	0,779	1,008	0,910	0,921	0,906	0,934
Center target 9	0,778	0,759	0,986	0,909	0,748	0,787	0,925	0,735
Center target 10	0,645	0,862	0,872	0,899	0,910	0,782	0,946	0,758
Center target 11	0,603	0,681	0,947	0,733	0,666	0,844	0,779	0,866
Center target 12	0,875	0,705	0,982	0,864	0,961	0,745	0,980	1,006
Center target 13	0,681	0,623	0,704	0,805	0,709	0,924	1,008	0,933
Center target 14	0,690	0,606	0,858	0,983	0,701	0,650	0,925	0,794
Center target 15	0,698	0,863	0,900	0,830	0,828	0,628	0,866	0,872
Center target 16	0,932	0,751	0,818	0,759	0,802	0,723	0,961	0,967
Center target 17	0,879	0,642	0,793	0,922	0,935	0,679	0,932	0,982
Center target 18	0,740	0,836	0,948	0,750	0,892	0,673	0,935	0,967
Center target 19	0,871	0,903	0,821	0,767	0,684	0,863	0,668	0,981
Center target 20	0,881	0,856	0,963	0,930	0,668	0,597	0,902	0,834
Center target 21	0,608	0,868	0,934	0,949	0,562	0,770	0,850	0,697
Center target 22	0,535	0,807	0,857	1,006	0,596	0,933	0,984	0,842
Center target 23	0,703	0,914	0,932	0,949	0,686	0,684	0,964	0,968
Center target 24	0,658	0,704	0,928	0,972	0,699	0,833	0,970	0,960
Center target 25	0,873	0,888	0,844	0,945	0,862	0,772	0,986	0,982
Center target 26	0,592	0,952	0,672	0,756	0,774	0,936	0,940	0,854
Center target 27	0,592	0,593	0,985	1,002	0,746	0,821	0,708	0,808
Center target 28	0,627	0,712	0,905	0,813	0,801	0,930	0,994	0,726
Center target 29	0,871	0,920	0,845	0,901	0,537	0,775	0,973	0,791
Center target 30	0,846	0,588	0,986	0,941	0,622	0,677	0,747	0,966
Center target 31	0,650	0,633	0,983	0,933	0,781	0,637	0,848	0,862
Center target 32	0,637	0,906	0,901	0,947	0,719	0,831	0,720	0,850
Average Center Target	0,730	0,788	0,881	0,888	0,762	0,799	0,890	0,879
PSD Center Target	0,108	0,119	0,094	0,083	0,111	0,104	0,098	0,092

Table A.7: Quantifying the average local field potentials (LFP) amplitude during horizontal prosaccades for session with DBS on and off in both hemispheres.

Horizontal Prosaccades Left Eye Gaze	DBS ON		DBS OFF	
	Right Hemisphere Average LFP Amplitude ($\mu V p$)	Left Hemisphere Average LFP Amplitude ($\mu V p$)	Right Hemisphere Average LFP Amplitude ($\mu V p$)	Left Hemisphere Average LFP Amplitude ($\mu V p$)
Right target 1	2,355	4,988	3,032	2,390
Right target 2	2,846	4,917	1,868	1,332
Right target 3	2,013	4,646	1,478	1,407
Right target 4	1,769	2,963	1,954	1,486
Right target 5	2,168	5,148	1,481	1,288
Right target 6	2,703	5,844	1,389	1,368
Right target 7	1,913	3,635	1,861	1,172
Right target 8	2,296	5,593	2,433	1,167
Right target 9	1,941	3,849	1,919	1,296
Right target 10	2,368	5,306	1,806	3,231
Right target 11	2,338	4,662	1,765	1,353
Right target 12	2,642	6,536	2,014	1,580
Right target 13	2,862	5,880	1,720	2,085
Right target 14	2,941	7,877	1,526	1,374
Right target 15	2,261	4,213	2,264	1,307
Right target 16	2,351	4,384	2,128	3,563
Average Right Target	2,360	5,027	1,915	1,712
PSD Right Target	0,346	1,150	0,402	0,712
Left target 1	2,559	3,694	1,404	0,950
Left target 2	1,786	3,717	2,685	1,555
Left target 3	2,291	5,718	2,447	1,442
Left target 4	2,177	4,269	2,328	1,193
Left target 5	3,011	5,300	2,575	2,913
Left target 6	2,357	5,162	1,269	1,235
Left target 7	1,883	3,744	2,263	3,097
Left target 8	1,758	2,914	1,402	1,921
Left target 9	1,861	5,010	1,344	1,504
Left target 10	2,359	4,183	3,504	3,106
Left target 11	2,570	5,299	1,733	1,258
Left target 12	2,422	3,909	1,600	3,384
Left target 13	1,766	4,453	1,620	1,292
Left target 14	2,040	3,581	2,166	3,490
Left target 15	2,789	4,882	1,564	1,550
Left target 16	2,499	4,521	1,795	3,116
Average Left Target	2,258	4,397	1,981	2,063
PSD Left Target	0,372	0,756	0,599	0,899

Table A.8: Quantifying the baseline period average LFP amplitude during horizontal prosaccades with DBS on and off in both hemispheres.

Horizontal Prosaccades Left Eye Gaze	DBS ON		DBS OFF	
	Right Hemisphere Average LFP Amplitude (μVp)	Left Hemisphere Average LFP Amplitude (μVp)	Right Hemisphere Average LFP Amplitude (μVp)	Left Hemisphere Average LFP Amplitude (μVp)
Center target 1	2,156	4,208	1,888	1,355
Center target 2	2,115	4,205	2,339	1,300
Center target 3	2,688	4,605	1,656	1,428
Center target 4	1,673	3,564	1,923	1,276
Center target 5	1,823	3,062	1,528	1,247
Center target 6	1,575	2,803	1,996	1,202
Center target 7	2,870	4,592	2,144	1,475
Center target 8	1,837	3,910	2,798	1,444
Center target 9	2,240	5,167	2,207	1,256
Center target 10	2,396	5,076	1,936	1,102
Center target 11	2,060	5,161	2,003	1,347
Center target 12	1,932	5,570	2,634	1,686
Center target 13	2,677	4,816	2,471	2,789
Center target 14	2,416	4,453	1,951	0,996
Center target 15	2,226	3,849	2,778	1,325
Center target 16	1,929	4,402	2,841	2,462
Center target 17	2,192	3,834	1,966	1,648
Center target 18	1,982	3,326	2,808	1,335
Center target 19	1,826	4,380	2,655	1,285
Center target 20	1,991	4,468	2,134	1,852
Center target 21	2,505	4,502	2,093	2,941
Center target 22	2,747	6,274	1,656	1,552
Center target 23	2,083	4,623	1,715	1,429
Center target 24	2,305	5,441	2,125	1,114
Center target 25	2,509	5,420	2,999	2,927
Center target 26	2,025	3,945	2,746	2,913
Center target 27	2,190	4,868	1,625	1,263
Center target 28	1,765	5,208	1,215	1,353
Center target 29	1,691	3,625	1,463	3,067
Center target 30	2,153	5,502	2,074	1,182
Center target 31	2,743	5,840	2,520	2,167
Center target 32	1,505	2,898	2,668	3,470
Average Center Target	2,151	4,487	2,174	1,725
PSD CenterTarget	0,355	0,849	0,461	0,690

Table A.9: Quantifying the average LFP amplitude during vertical prosaccades for session with DBS on and off in both hemispheres.

Vertical Prosaccades Left Eye Gaze	DBS ON		DBS OFF	
	Right Hemisphere Average LFP Amplitude (μVp)	**Left Hemisphere** Average LFP Amplitude (μVp)	**Right Hemisphere** Average LFP Amplitude (μVp)	**Left Hemisphere** Average LFP Amplitude (μVp)
Up target 1	2,541	4,427	2,882	2,358
Up target 2	2,753	5,499	1,915	1,677
Up target 3	2,053	4,597	1,696	2,279
Up target 4	2,311	4,505	2,208	3,452
Up target 5	2,661	3,992	1,747	1,390
Up target 6	2,006	4,747	1,759	1,572
Up target 7	1,914	3,221	2,594	1,390
Up target 8	1,613	2,651	1,477	1,739
Up target 9	2,190	3,900	3,042	1,727
Up target 10	1,901	3,154	2,507	1,512
Up target 11	2,154	4,904	2,132	1,506
Up target 12	1,796	2,207	1,726	1,561
Up target 13	2,189	4,624	1,601	1,114
Up target 14	1,954	5,011	1,724	1,555
Up target 15	2,328	4,364	2,153	3,863
Up target 16	1,870	2,828	1,816	0,977
Average Up Target	2,140	4,039	2,061	1,854
PSD Up Target	0,308	0,924	0,457	0,763
Down target 1	2,695	5,907	1,568	1,583
Down target 2	2,438	4,868	2,476	1,348
Down target 3	2,749	5,684	2,373	1,637
Down target 4	1,998	2,753	2,299	1,740
Down target 5	2,514	5,087	1,721	3,510
Down target 6	2,403	4,739	1,922	1,460
Down target 7	1,990	3,965	2,132	1,592
Down target 8	1,730	2,808	2,026	1,466
Down target 9	2,737	5,202	2,360	1,285
Down target 10	1,912	4,209	3,544	3,296
Down target 11	2,384	2,805	2,489	3,471
Down target 12	2,277	4,538	2,137	1,586
Downtarget 13	1,847	2,910	2,297	2,271
Down target 14	1,962	4,272	2,839	3,562
Down target 15	1,939	4,750	1,918	1,365
Down target 16	2,017	2,460	2,086	1,614
Average Down Target	2,224	4,185	2,262	2,049
PSD Down Target	0,329	1,084	0,449	0,843

Table A.10: Quantifying the baseline period average LFP amplitude during vertical prosaccades with DBS on and off in both hemispheres.

Vertical Prosaccades Left Eye Gaze	DBS ON		DBS OFF	
	Right Hemisphere Average LFP Amplitude (μVp)	Left Hemisphere Average LFP Amplitude (μVp)	Right Hemisphere Average LFP Amplitude (μVp)	Left Hemisphere Average LFP Amplitude (μVp)
Center target 1	2,127	5,155	2,058	1,619
Center target 2	2,226	4,368	2,169	1,547
Center target 3	2,310	5,388	1,525	1,418
Center target 4	2,175	5,233	1,999	3,131
Center target 5	2,115	2,968	2,168	1,603
Center target 6	2,242	4,609	2,514	2,876
Center target 7	1,814	2,629	2,272	3,460
Center target 8	2,112	3,749	1,896	1,531
Center target 9	2,616	4,610	1,977	1,233
Center target 10	3,131	4,488	2,103	1,542
Center target 11	2,227	3,571	1,866	1,287
Center target 12	2,683	2,725	2,500	1,164
Center target 13	2,546	3,915	2,258	3,362
Center target 14	1,904	4,053	2,503	1,665
Center target 15	1,744	4,945	1,933	3,336
Center target 16	2,176	3,024	1,821	1,775
Center target 17	1,721	2,929	2,430	1,516
Center target 18	2,018	3,100	2,047	1,444
Center target 19	1,736	4,527	2,429	1,918
Center target 20	2,684	4,633	2,464	1,297
Center target 21	2,384	4,376	1,640	1,481
Center target 22	2,177	4,305	2,288	3,237
Center target 23	2,281	2,730	1,887	1,529
Center target 24	1,793	2,877	2,108	2,098
Center target 25	2,602	5,373	2,554	1,259
Center target 26	2,294	4,202	2,771	1,565
Center target 27	1,847	3,728	1,920	3,253
Center target 28	2,167	3,887	2,350	1,381
Center target 29	1,241	3,733	1,972	3,421
Center target 30	1,515	3,100	2,109	1,834
Center target 31	2,380	4,145	1,847	3,223
Center target 32	2,184	3,054	2,527	1,460
Average Center Target	2,162	3,942	2,153	2,014
PSD CenterTarget	0,373	0,829	0,290	0,803